Article

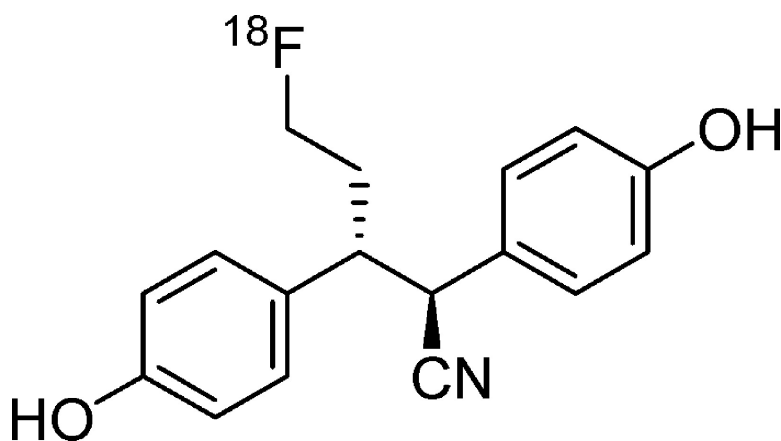# Synthesis of an Estrogen Receptor β-Selective Radioligand: 5-[F]Fluoro-(2R*,3S*)-2,3-bis(4-hydroxyphenyl)pentanenitrile and Comparison of in Vivo Distribution with 16□-[F]Fluoro-17β-estradiol

Jeongsoo Yoo, Carmen S. Dence, Terry L. Sharp, John A. Katzenellenbogen, and Michael J. Welch

More About This Article

Additional resources and features associated with this article are available within the HTML version:

- Supporting Information
- Links to the 2 articles that cite this article, as of the time of this article download
- Access to high resolution figures
- Links to articles and content related to this article
- Copyright permission to reproduce figures and/or text from this article

View the Full Text HTML

Synthesis of an Estrogen Receptor *β*-Selective Radioligand: 5-[18F]Fluoro-(2*R**,3*S**)-2,3-bis(4-hydroxyphenyl)pentanenitrile and Comparison of in Vivo Distribution with 16α-[18F]Fluoro-17*β*-estradiol

Jeongsoo Yoo,[†,§] Carmen S. Dence,[†] Terry L. Sharp,[†] John A. Katzenellenbogen,[‡] and Michael J. Welch[†,*]

Mallinckrodt Institute of Radiology, Washington University School of Medicine, Campus Box 8225, 510 South Kingshighway Boulevard, St. Louis, Missouri 63110, and Department of Chemistry, University of Illinois, Urbana, Illinois 61801

Received February 8, 2005

Estrogen receptor *β* (ER*β*), a less active ER subtype that appears to have a restraining effect on the more active ERα, could be a factor that determines the level of estrogen action in certain estrogen target tissues. ER*β* is found in breast cancer, and its levels relative to ERα decline with disease progression. Thus, the independent quantification of ERα and ER*β* levels in breast cancer by imaging might be predictive of responses to different hormone therapies. To develop an imaging agent for ER*β*, we synthesized a fluoroethyl analogue of DPN (2,3-bis(4-hydroxyphenyl)propanonitrile), a known ER*β*-selective ligand. This analogue, FEDPN (5-fluoro-(2*R**,3*S**)-2,3-bis(4-hydroxyphenyl)pentanenitrile), has an 8.3-fold absolute affinity preference for ER*β*. [18F]Fluoride-labeled FEDPN was prepared from a toluenesulfonate precursor, which provided [18F]FEDPN with a specific activity greater than 3100 Ci/mmol after HPLC purification. Biodistribution studies in immature female rats using estradiol as a blocking agent revealed specific uptake of [18F]FEDPN in the uterus and ovaries. Experiments using ERα- and ER*β*-knockout mice demonstrated the expected ERα-subtype dependence in the tissue uptake of the known 16α-[18F]fluoro-17*β*-estradiol ([18F]FES), which has a 6.3-fold preference for ERα. The tissue uptake of [18F]FEDPN in the ER knockout mice showed some evidence of mediation by ER*β*, but the levels of specific uptake of this agent were relatively modest. Based on our results, imaging of ERα can be done effectively with [18F]FES, but imaging of ER*β* will likely require agents with more optimized ER*β* binding affinity and selectivity than [18F]FEDNP.

Introduction

The estrogen receptor (ER), a ligand-regulated transcription factor, is the principal mediator of genomic responses to estrogens, and it plays an important regulatory role in reproductive and other tissues.[1] Tumors derived from estrogen target tissues, such as breast tumors, often retain receptors for estrogens and in many cases are sensitive to antiestrogens, such as tamoxifen and raloxifene, and assays of ER levels in tumors are used to assess the prospects for a favorable clinical response to hormone therapy.[2,3] Previously, we demonstrated that ER-positive breast tumors can be imaged by positron emission tomography (PET) using F-18-labeled estrogens,[4−7] and that these images can be used to provide an early assessment of response to hormone therapy.[8,9]

Even though it was originally believed that there was only one ER, a second ER gene was reported in 1996.[10] This gene is called ER*β* to distinguish it from the long-known ER, which is now called ERα. ERα and ER*β* subtypes have rather different tissue distributions.[11−13] Tissues that have high ER*β* levels include prostate, testes, ovaries, gastrointestinal tract, lung, bladder, hematopoetic and central nervous systems, and certain regions of the brain, whereas ERα predominates in the uterus, breast, kidney, liver, and heart. Many tissues contain both ERα and ER*β*, such as breast, epididymis, thyroid, adrenal, bone, and certain other regions of the brain.[14]

The response of ERα and ER*β* to estrogens of different structure can vary considerably. In addition, because the gene transcriptional activity of ER*β* is generally less than that of ERα, ER*β* is thought to act as a proliferative "brake" on ERα.[15] Thus, the relative levels of ERα vs ER*β* in a particular tissue are likely to determine how much activity an estrogen will have in that tissue and how it will respond to ligands of different structures.

Although normal breast tissue contains both ERα and ER*β*, in breast tumors, ER*β* levels decline relative to ERα as this disease progresses and the cancer becomes more malignant.[16−20] Thus, an independent determination of ERα and ER*β* levels in breast tumors might provide a useful molecular assessment of the stage of the disease and its sensitivity to various endocrine therapies, information that could help in the selection of the best alternative therapies for an individual breast cancer patient. It would be particularly convenient if this quantification of ERα and ER*β* levels could be done noninvasively by PET imaging.
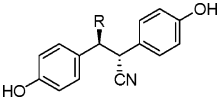
We have recently found that 2,3-bis(4-hydroxyphenyl)propionitrile (DPN) is an agonist for both ER subtypes, but has a 70-fold higher relative binding affinity (RBA, that is, ER*β* vs ERα binding relative to the affinity of estradiol) and 78-fold higher potency (based

* Corresponding author. Tel: 1 314 362 8436, Fax: 1 314 362 8399, e-mail: welchm@wustl.edu.
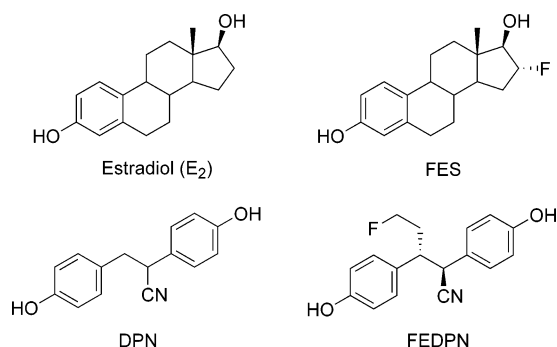† Washington University.
‡ University of Illinois.
§ Department of Molecular Medicine, Kyungpook National University School of Medicine, Dongin-dong 2-ga, Joong-gu, Daegu 700-422, Korea.

Table 1. Relative Binding Affinities (RBA)[a] of DPN Derivatives for the ERα and ERβ[21]

	relative binding affinity (E_2= 100)			absolute
R	ERα	ERβ	ERβ/ERα[b]	ERβ/ERα ratio[b]
H (DPN)	0.25 ± 0.15	18 ± 2	72	29
CH$_3$	1.7 ± 0.3	48 ± 3	27	11
CH$_2$CH$_3$	17 ± 5	75 ± 6	4	1.6
CN (meso)	0.55 ± 0.07	29 ± 7	53	21

[a] Determined by a competitive radiometric biding assay with [^{3}H]estradiol using full-length human ERα and ERβ. Values are reported as the mean ± SD. [b] These ERα/ERβ ratios are corrected for the fact that the tracer, estradiol, binds to the two ER subtypes with different affinities (K_d (ERα) = 0.2 nM; K_d (ERβ) = 0.5 nM).

on EC$_{50}$ values) in transcription assays with ERβ.[21] To further investigate the ERβ affinity-selective charac-

teristic of DPN, we prepared a series of DPN analogues (Table 1).[21] Because of their very high ERβ affinity preference, DPN and its analogues appeared to be good starting points for development of radiopharmaceuticals for imaging only ERβ. Fluorine-18 is an excellent radionuclide for in vivo imaging with PET.[22]

Herein, we report the synthesis of 5-[^{18}F]fluoro-($2R^*,3S^*$)-2,3-bis(4-hydroxyphenyl)pentanenitrile ([^{18}F]-FEDPN), its labeling with F-18 and an assessment of its selectivity for in vivo imaging of ERβ. Tissue distribution studies of [^{18}F]FEDPN were performed in rats as well as in mice in which either ERα or ERβ had been knocked out, and its uptake in these mice is compared with that of the known (and ERα preferential) imaging agent 16-[^{18}F]fluoro-17β-estradiol ([^{18}F]FES). In these animal models, the patterns and time course of tissue distribution of both [^{18}F]FEDNP and of [^{18}F]-FES were found to reflect, to some degree, their affinity preferences for ERβ and ERα, respectively. The ERα-selective uptake of [^{18}F]FES, however, is more pronounced than the ERβ-selective uptake of [^{18}F]FEDNP.

Results

Synthesis of an Unlabeled Standard of FEDPN. From a series of DPN analogues (Table 1) with good ERβ/ERα selectivity, ($2R^*,3S^*$)-5-fluoro-2,3-bis(4-hydroxyphenyl)pentanenitrile (**5**) was chosen as a target compound for ERβ imaging. It is a fluorine analogue of ($2R^*,3S^*$)-2,3-bis(4-hydroxyphenyl)pentanenitrile (R = Et in Table 1), which has a relative binding affinity (RBA) value of 17 ± 5 for ERα and 75 ± 6 for ERβ (estradiol = 100 for both ERα and ERβ).
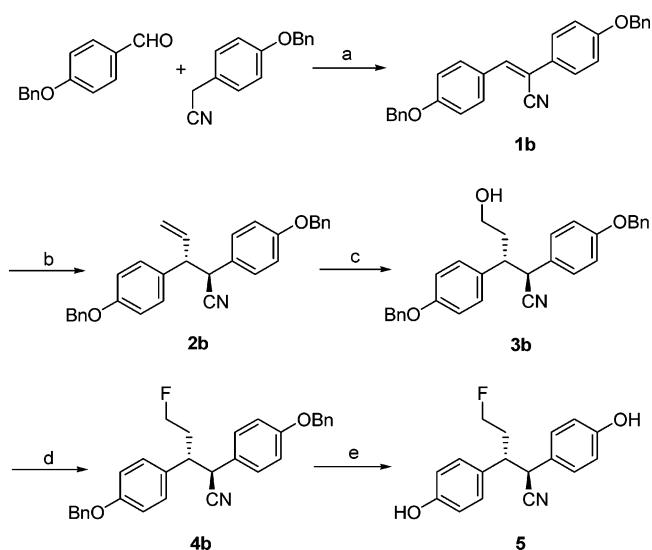
Scheme 1[a]
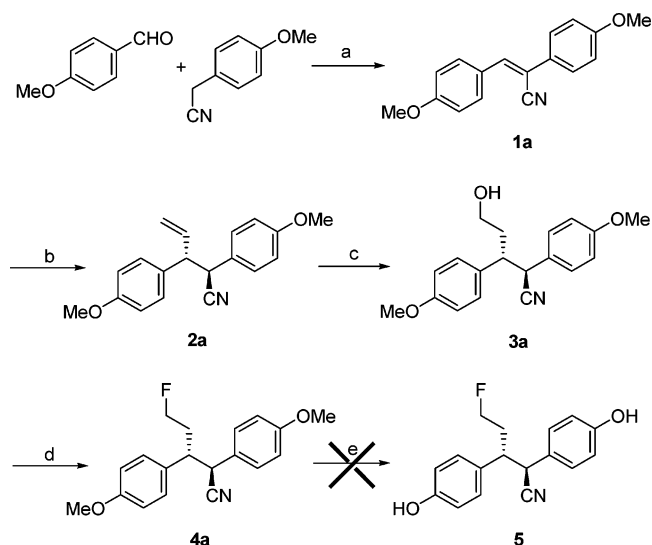
[a] Reagents and conditions: (a) NaOMe, EtOH; (b) CH$_2$=CHMgBr, CuI, THF; (c) i) BH$_3$·THF, ii) NaOH, H$_2$O$_2$; (d) DAST, CH$_2$Cl$_2$; (e) BBr$_3$, CH$_2$Cl$_2$, −76 °C.

It is of note that the fluorine analogue of DPN itself, 3-fluoro-2,3-bis(4-hydroxyphenyl)propanenitrile, was not selected because it was expected to undergo rapid defluorination under physiological conditions by a facile elimination mechanism.[23−25] The cyanide group in the fourth DPN analogue could be labeled by C-11 (R = CN in Table 1); however, the half-life of C-11 (20 min) was considered to be too short for breast cancer imaging.

In our first approach, the methoxy-protected phenol compounds 4-(methoxy)phenylacetonitrile and *p*-anisaldehyde were used as starting materials to prepare the target compound, ($2R^*,3S^*$)-5-fluoro-2,3-bis(4-hydroxyphenyl)pentanenitrile (Scheme 1). α-Cyanostilbene **1a** was prepared by the condensation of the arylaldehyde and arylacetonitrile in quantitative yield by modification of a previous method.[21] The product that precipitated was collected on a glass frit and washed by ethanol. The filtrate was concentrated under vacuum in order to remove water produced during condensation reaction, dry EtOH was added up to an original solvent volume when necessary, and the same amount of NaOMe was added into the mixture as new base. The second precipitate was collected and washed by ethanol. In this manner, the yield was quantitative, which is much higher than that previously reported (72%).

The vinyl group was introduced at β-position with high diastereoselectivity by the conjugate addition of the Grignard reagent in the presence of CuI. Pure erythro diastereomer was obtained by repeated recrystallization (1 h) from refluxing ethyl acetate/hexane (1:1). Stereochemical assignment was based on spectroscopic analogy to the β-ethyl analogue[21] (R = Et in Table 1). Hydroboration of the vinyl group with BH$_3$·THF followed by oxidation gave the primary alcohol, ($2R^*,3S^*$)-5-hydroxy-2,3-bis(4−methoxyphenyl)pentanenitrile (**3a**), in moderate yield. The alcohol group of compound **3a** was then replaced by fluoride directly using (diethylamino)sulfur trifluoride (DAST) to give ($2R^*,3S^*$)-5-fluoro-2,3-bis(4−methoxyphenyl)pentanenitrile (**4a**). However, attempts to deprotect the methyl ether to give unlabeled FEDPN (**5**) failed to do so without also

Scheme 2[a]

[a] Reagents and conditions: (a) NaOMe, EtOH, reflux; (b) CH$_2$=CHMgBr, CuI, THF; (c) i) BH$_3$·THF, ii) NaOH, H$_2$O$_2$; (d) DAST, CH$_2$Cl$_2$; (e) H$_2$, Pd/C.

cleaving the C−F bond (Reagents including BBr$_3$,[26,27] BF$_3$, AlCl$_3$,[28] pyridine·HCl,[29,30] and CH$_3$SO$_3$H[31] were tried under various reaction conditions.) Thus, we decided to change to a more easily cleaved protecting group.

In our second synthesis (Scheme 2), a benzyl group was chosen to protect the phenol because it can easily be removed by hydrogenation. The condensation reaction between 4-(benzyloxy)benzaldehyde and 4-(benzyloxy)phenylacetonitrile was carried out in refluxing ethanol because of low initial solubility at room temperature. The yield was increased to nearly quantitative by continuous removal of water and addition of more base. The vinyl group was introduced at β-position using vinyl Grignard reagent with copper catalysis, and pure *erythro*-**2b** was obtained by repeated recrystallization (1 h) from refluxing ethanol. Hydroboration followed by oxidation and fluorination of primary alcohol were achieved by employing similar reaction conditions as those in Scheme 1 to give (2*R**,3*S**)-2,3-bis(4-(benzyloxy)phenyl)-5-fluoropentanenitrile (**4b**). Deprotection of the benzyl groups was successfully achieved by a typical hydrogenolysis reaction over Pd/C catalyst to give (2*R**,3*S**)-5-fluoro-2,3-bis(4-hydroxyphenyl)pentanenitrile (**5**). Ethyl acetate was used as a solvent because of the very poor solubility of compound **4b** in alcohol. The presence of fluorine was clearly seen from ^{1}H and ^{13}C NMR data through the coupling of fluorine with the proton and carbon-13 signals. Compound **5** was further characterized by high-resolution mass spectrometry.

Even though phenol benzyl ether could be cleaved under mild conditions, the deprotection took 4 h. The benzyl group is, therefore, not optimal as a phenol protecting group for labeling FEDPN with F-18, because of the relatively short half-life of F-18 ($t_{1/2}$ = 110 min). Of various other phenol protecting groups such as methoxymethyl, methanesulfonate, and *tert*-butyldimethylsilyl, the methoxyethoxymethyl (MEM) group was selected because it is stable under base conditions, yet can be removed very rapidly under relatively mild acid conditions.[32]

Scheme 3[a]
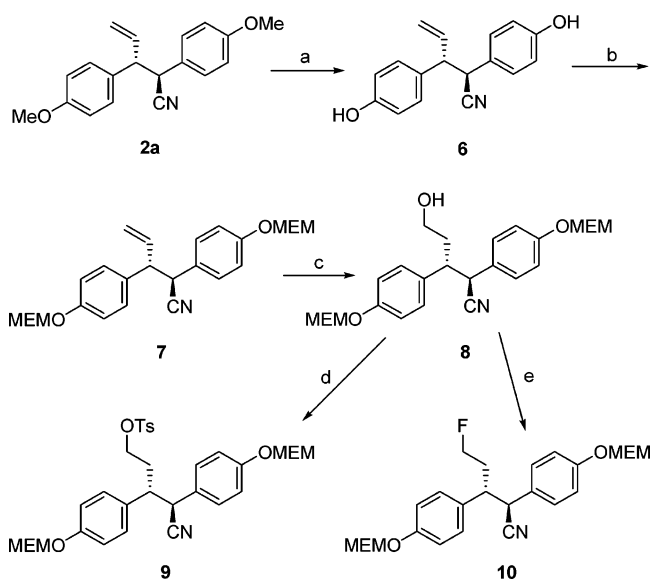
[a] Reagents and conditions: (a) BBr$_3$, CH$_2$Cl$_2$, 0 °C; (b) MEMCl, *i*Pr$_2$Net, CH$_2$Cl$_2$; (c) i) BH$_3$·THF, ii) NaOH, H$_2$O$_2$; (d) TsCl, py, CH$_2$Cl$_2$; (e) DAST, CH$_2$Cl$_2$.

The methyl ethers in compound **2a** were cleaved by overnight treatment of BBr$_3$, affording (2*R**,3*S**)-2,3-bis(4-hydroxyphenyl)pent-4-enenitrile (**6**) in quantitative yield (Scheme 3). The free phenol groups in **6** then reprotected with MEM groups, using MEM chloride and *N,N*-diisopropylethylamine, to give (2*R**,3*S**)-2,3-bis(4-((2-methoxyethoxy)methyl)phenyl)pent-4-enenitrile (**7**). Hydroboration with BH$_3$·THF followed by treatment with aqueous NaOH/H$_2$O$_2$ converted the alkene in this compound to the terminal alcohol. The hydroxy group in **8** was converted to the tosylate group by treatment with *p*−toluenesulfonyl chloride and pyridine to give (3*R**,4*S**)-3,4-bis(4-((2-methoxyethoxy)methyl)phenyl)-4-cyanobutyl 4−methylbenzenesulfonate (**9**), which is ready for labeling with [^{18}F]fluoride ion. The hydroxy group in compound **8** was converted to fluorine using DAST to give (2*R**,3*S**)-2,3-bis(4-((2-methoxyethoxy)methyl)phenyl)-5−fluoropentanenitrile (**10**), which is used as standard for [^{18}F]**10**.

Binding Affinities of FES and FEDPN. Binding affinities of FES and FEDPN were determined by a competitive radiometric binding assay with [^{3}H]estradiol as tracer, using purified full-length human ERα and ERβ, as previously described.[33,34] Affinities from these competitive binding assays are expressed as relative binding affinity (RBA) values, that is, relative to the affinity of estradiol, which is 100% by definition (Table 2).

One should note that affinity calculations based on relative binding affinity (RBA) values (i.e., compared to estradiol) do not reflect the fact that the tracer, estradiol, binds to ERα and ERβ with somewhat different affinities (K_d: 0.2 nM for ERα and 0.5 nM for ERβ). Therefore, in both Tables 1 and 2 we express the binding affinity ratios both in terms of relative affinities (i.e., based on RBA values, left) and absolute affinities (right), the latter being corrected for the 2.5-fold difference in estradiol affinity for ERα vs ERβ.

The binding affinity of FES is relatively high for both ERα and ERβ subtypes, being in the nanomolar range.

Table 2. Relative Binding Affinities (RBA)[a] of FES and FEDPN

| | RBA (%)[a] | | | absolute |
ligand	ERα	ERβ	ERα/ERβ	ERα/ERβ ratio[b]
estradiol	100	100	[1.00]	2.5[b]
FES	54.9 ± 15	22.0 ± 1.6	2.5	6.3
FEDPN	0.42 ± 0.09	8.74 ± 1.87	0.048	0.12

[a] Values are reported as the mean range. [b] These ERα/ERβ ratios are corrected for the fact that the tracer, estradiol, binds to the two ER subtypes with different affinities (K_d (ERα) = 0.2 nM; K_d (ERβ) = 0.5 nM).

Scheme 4[a]
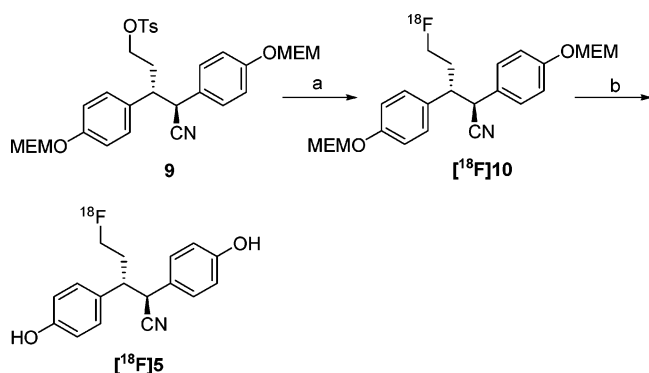
[a] Reagents and conditions: (a) [18F]-, K$_2$CO$_3$, K222, MW; (b) 3M HCl, 110 °C, 5 min.

FES showed 2.5 times higher RBA selectivity for ERα over ERβ (55 vs 22), thus giving it a 6.3-fold absolute affinity preference for ERα.

The affinity of FEDPN for ERα is less than 0.5% that of estradiol, while its affinity for ERβ is around 10% of estradiol, giving an ERβ affinity selectivity of 21 based on RBA comparison or 8.3 in terms of absolute affinities. Thus, the fluorine substituent decreased the binding affinity considerably compared to the non-fluorine substituted analogue, β-ethylated DPN (R = Et in Table 1), which has an RBA of 75 for ERβ and 17 for ERα, corresponding to an ERβ RBA preference of only 4.[21] Thus, although the RBA of FEDPN is about 10-fold less on ERβ compared to that of β-ethylated DPN, its affinity for ERα is even more reduced, giving it an RBA selectivity for ERβ of 21, which is actually higher than that of the ethyl-substituted analogue.

In general, an increase in steric bulk at the β position next to the nitrile in DPN analogues (Table 1) tends to raise ligand binding affinity for both receptors while decreasing ERβ/ERα selectivity ratio. However, addition of a fluorine substituent, considered to be between hydrogen and methyl in size,[32] onto the β ethyl group causes a reverse effect, lowering RBA for both ER subtypes but raising ERβ selectivity. This is likely the result of introducing a more polar function near the center of the ligand.

Because of its reasonable ERβ/ERα selectivity (21-fold based on relative affinities, 8.3, based on absolute affinities), we labeled FEDPN with fluorine-18, with the objective of developing a PET imaging agent that would be specific for ERβ.

Radiochemical Synthesis of [18F]FEDPN. Scheme 4 illustrates the microwave-mediated two-step radiosynthesis of [18F]FEDPN. Fluorine-18 obtained from proton bombardment of oxygen-18 enriched water was treated by ion-exchange resin (BioRad AG-1 × 8) to produce metal ion-free fluoride, and the [18O]-water was recycled. This material was converted to [18F]KF/Kryptofix-222 by the addition of Kryptofix-222 and careful azeotropic drying with acetonitrile. The activity was then resolubilized in MeCN and transferred to a Pyrex tube containing diastereomerically pure tosylate precursor **9**.

The nucleophilic substitution of the tosyl group by [18F]fluoride ion was optimized by varying the fluoride source, the amount of substrate and the microwave irradiation time. The incorporation yield was determined by radio-TLC where the R_f value of [18F]**10** matched well with that of the unlabeled compound **10** (0.49 vs 0.50). The substrate **9** was very sensitive to base and degraded quickly with heating during fluorination. Heating in a specially designed microwave cavity for 35 s resulted in the highest labeling yield, whereas longer heating or the repeated cycles of irradiation and cooling decreased incorporation. Microwave dielectric heating is known to give cleaner reaction mixtures because of decreased reactant decomposition and shorter reaction time compared to conventional heating.[35]

The fluoride source was critical to effective labeling. Maximal incorporation yield was less than 4% when non-ion exchange-treated water was used as the [18F] ion source. The tiny amount of metal ions in nontreated water appeared to accelerate decomposition of the substrate before displacement of tosylate by fluoride ion. When nontreated water was used, more than 70% of the toluenesulfonate precursor was degraded right after the incorporation reaction. (as determined by HPLC) When less than 2 mg of substrate was used, incorporation yield also decreased significantly compared to using more than 3 mg of substrate (7.2 ± 3.0% vs 23.0 ± 6.9%), presumably also due to decomposition of substrate.

After the replacement of tosylate by fluorine-18 ion, the MEM protecting groups were deprotected within 3 min by treatment with 3 M HCl at 110 °C to give final product [18F]FEDPN. The R_f value (0.58) of [18F]FEDPN determined by radio−TLC matched exactly that of unlabeled **5**. The radiochemical yield decreased by about 30% (determined by radio-TLC) following deprotection, indicating cleavage of the C−F bond during the acid hydrolysis. Only the peaks for [18F]FEDPN and free fluoride were seen on radio−TLC.

Solid-phase purification to remove free fluoride was performed by using an OASIS HLB cartridge, as described previously.[36] Purification of the final tracer was accomplished by reverse phase HPLC. The desired fractions were collected by monitoring the radioactivity trace, since the UV absorption of the final product [18F]-FEDPN was below the detection limit. The collected fractions were evaporated under reduced pressure and then reconstituted in 10−20% ethanol/saline mixture for further studies.

The total radiosynthesis time including HPLC purification took less than 110 min, and it proceeded with a radiochemical yield of 3.4 ± 3.0% (n = 4, decay corrected). The overall radiochemical yield was low, but is in keeping with multistep radiofluorination reactions.[37] The radiochemical purity determined by reverse phase analytical HPLC was greater than 99%. Based on the detection limit measurement of cold FEDPN mass by the UV detector, the specific activity was

Table 3. Biodistribution of [18F]FEDPN in Immature Female Sprague−Dawley Rats[a]

organ	30 min	1 h	1 h block	2 h
blood	0.64 ± 0.31	0.55 ± 0.20	0.30 ± 0.10	0.24 ± 0.07
lung	0.71 ± 0.20	0.44 ± 0.10	0.27 ± 0.10	0.19 ± 0.07
liver	1.42 ± 0.29	1.51 ± 0.15	0.76 ± 0.17	0.62 ± 0.14
spleen	0.31 ± 0.10	0.16 ± 0.04	0.10 ± 0.05	0.06 ± 0.01
kidney	2.00 ± 0.60	1.75 ± 0.37	1.01 ± 0.38	0.97 ± 0.21
muscle	0.57 ± 0.14	0.22 ± 0.00	0.20 ± 0.08	0.09 ± 0.01
fat	0.57 ± 0.22	0.37 ± 0.16	0.21 ± 0.14	0.10 ± 0.06
heart	0.49 ± 0.14	0.29 ± 0.07	0.19 ± 0.08	0.11 ± 0.02
bone	2.12 ± 0.49	2.22 ± 0.26	1.82 ± 0.44	1.88 ± 0.11
uterus	0.95 ± 0.23	0.74 ± 0.29	0.34 ± 0.15	0.28 ± 0.11
ovaries	0.93 ± 0.33	0.67 ± 0.18	0.26 ± 0.11	0.21 ± 0.06
thymus	0.52 ± 0.09	0.29 ± 0.11	0.16 ± 0.07	0.08 ± 0.01

[a] Data are expressed as the %ID/g ± SD with five animals per data point.

calculated to be >3100 Ci/mmol (by UV absorption) at the end of synthesis.

Biodistribution Studies Using Immature Female Sprague−Dawley Rats. Immature female rats are useful for screening estrogen receptor ligands because they have low endogenous estrogens and yet have ER-rich target tissues (uterus and ovaries).[32] By using immature female rats (<25 days old), the effect of endogenous estradiol can be essentially obviated because the estrus cycle in rat begins around 30 days after birth.[38] Radiochemically pure [18F]FEDPN ([18F]**5**), reconstituted in 20% ethanol/saline, was injected into immature female Sprague−Dawley rats. Due to the low solubility of estradiol in aqueous solution, 20% ethanol/saline (150 μL) was used to dissolve estradiol (8 μg) for the blocking study.

Table 3 presents the uptake of [18F]FEDPN in selected tissues of immature female Sprague−Dawley rats at 30 min, 1 h (control and block by E$_2$) and 2 h ($n = 5$ at each time point). Highest uptake was found in bone at all time points including in estradiol blocked animals, indicative of the uptake of free [18F]fluoride ions produced by the in vivo metabolism of the radio−labeled compound.[37,39] Bone activity remained within the standard deviations at the three time points, indicating that degradation of [18F]FEDPN occurred within 30 min. The percentage of injected dose per gram (%ID/g) in the kidney was higher than that in liver at all three time points.

Except for these three tissues, the highest %ID/g was found in the estrogen receptor-rich organs such as ovaries and uterus. The uptake of [18F]FEDPN in the uterus at 30 min was comparable with that of ovaries at 30 min (0.95 vs 0.93), and slightly higher than that of ovaries at 1 and 2 h. The uterus/muscle ratio was 1.7 at 30 min and increased to more than 3 at 1 and 2 h time points. The ovary/muscle ratio was 1.6 at 30 min, 3.1 at 1 h and 2.3 at 2 h. The uterus/blood ratio was highest at 30 min (1.5) and decreased to 1.4 at 1 h and 1.2 at 2 h, while the ovaries/blood ratio was 1.5 at 30 min and 1.2 at 1 h, but dropped below 1 at 2 h postinjection. Even though the uterus and ovary uptake is not high, ratios with muscle and blood are suggestive of the fact that [18F]FEDPN uptake in these tissues might be the result of its binding to the estrogen receptor.

More direct evidence of the estrogen receptor-mediated uptake of [18F]FEDPN comes from comparisons with uptake in estradiol-blocked rats (Figure 1). Estradiol blocked the uptake of [18F]FEDPN in the estrogen receptor-rich organs; uterus and ovary were blocked by 54% and 61%, respectively, which is much greater than the blockage in ER-negative tissues, such as the 9% and 18% decrease in muscle and bone, respectively. However, clearance organs such as liver and kidney also showed lower uptake in the blocking study compared to control (0.76 vs 1.51 in liver; 1.01 vs 1.75 in kidney). Although the blocking effects are modest, the results of this study are consistent with the uptake of [18F]FEDPN in estrogen-rich organs being mediated by specific receptor binding; the modest level of these effects is consistent with the limited binding affinity of this compound for the ERs.

Biodistribution Studies Using Estrogen Receptor Knockout Mice. To determine whether the tissue distribution of [18F]FEDPN reflects its preferential binding affinity for the ERβ subtype, a second biodistribution study was carried out using two different sets of mice. In these studies, uptake of [18F]FES, an established ER imaging agent, was compared to uptake of [18F]FEDPN, the ERβ preferential ligand.

The estrogen receptor- knock-out (αERKO) mouse model was created by disrupting the ERα gene by gene
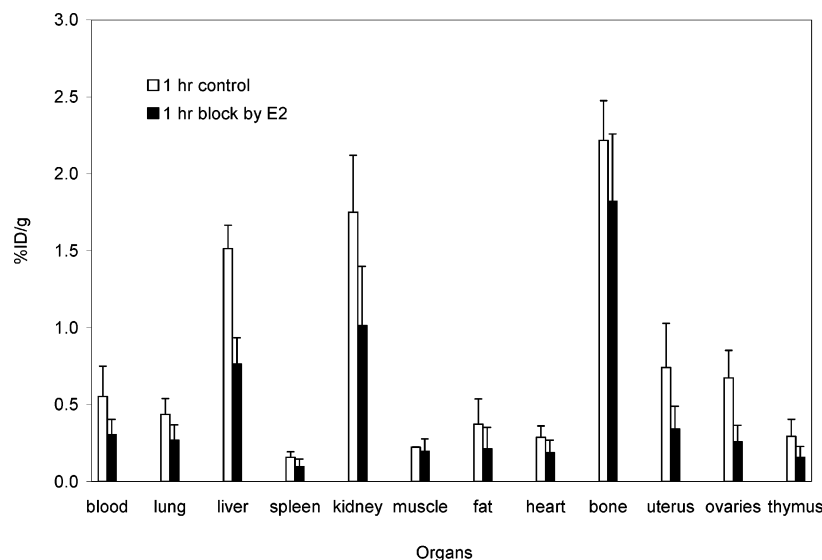
Figure 1. Comparison of tissue biodistribution data of [18F]FEDPN in control rats vs estradiol-blocked rats at 1 h postinjection.

Table 4. Biodistribution of [^{18}F]FES in αERKO and βERKO Mice[a]

| | αERKO | | | βERKO | | | |
organ	30 min	1 h	2 h	30 min diestrus[b]	30 min[c]	1 h[c]	2 h[c]
blood	0.65 ± 0.15	0.21 ± 0.02	0.12 ± 0.01	0.73 ± 0.15	0.67 ± 0.16	0.30 ± 0.01	0.16 ± 0.04
lung	2.19 ± 0.52	0.39 ± 0.08	0.17 ± 0.02	3.57 ± 0.57	3.74 ± 0.40	1.48 ± 0.22	0.54 ± 0.08
liver	7.47 ± 1.32	5.24 ± 0.19	3.67 ± 0.85	7.91 ± 0.87	9.45 ± 2.49	5.85 ± 1.62	4.54 ± 1.49
spleen	0.59 ± 0.14	0.19 ± 0.02	0.18 ± 0.10	1.29 ± 0.14	1.40 ± 0.19	0.91 ± 0.21	0.37 ± 0.04
kidney	2.46 ± 0.46	1.07 ± 0.12	0.72 ± 0.07	4.44 ± 0.67	3.83 ± 0.61	2.14 ± 0.37	1.05 ± 0.23
muscle	0.77 ± 0.27	0.18 ± 0.05	0.11 ± 0.04	1.89 ± 0.41	1.70 ± 0.15	1.29 ± 0.27	0.54 ± 0.07
fat	1.51 ± 0.36	0.14 ± 0.03	0.09 ± 0.01	2.31 ± 0.39	2.01 ± 0.15	1.07 ± 0.25	0.41 ± 0.05
heart	0.62 ± 0.15	0.15 ± 0.03	0.10 ± 0.01	0.95 ± 0.09	1.04 ± 0.20	0.46 ± 0.04	0.20 ± 0.04
brain	0.41 ± 0.05	0.07 ± 0.04	0.03 ± 0.01	0.81 ± 0.26	0.71 ± 0.10	0.35 ± 0.03	0.14 ± 0.02
bone	0.44 ± 0.05	0.24 ± 0.06	0.23 ± 0.12	1.26 ± 0.24	1.28 ± 0.17	1.08 ± 0.16	0.53 ± 0.10
uterus	2.40 ± 0.49	0.82 ± 0.25	0.36 ± 0.03	18.86 ± 0.11	8.34 ± 2.91	9.81 ± 3.42	9.23 ± 3.04
ovaries	2.52 ± 0.42	0.49 ± 0.04	0.18 ± 0.01	6.60 ± 2.68	6.54 ± 0.58	5.61 ± 1.29	3.40 ± 0.79
thymus	0.68 ± 0.18	0.21 ± 0.02	0.10 ± 0.01	1.65 ± 0.37	1.38 ± 0.19	0.92 ± 0.14	0.38 ± 0.07

[a] Data are expressed as the %ID/g ± SD with three animals per data point. [b] Mice were in nonestrus stage ($n = 2$). [c] Mice were in estrus ($n = 3$ per each time point).

Table 5. Uptake Ratios of βERKO/αERKO of [^{18}F]FES and [^{18}F]FEDPN in Uterus and Ovaries

| | βERKO/αERKO in uterus[c] | | | βERKO/αERKO in ovaries[c] | | |
ligand	30 min	1 h	2 h	30 min	1 h	2 h
[^{18}F]FES[a]	3.48 ± 0.57	12.0 ± 1.4	25.4 ± 1.8	2.60 ± 0.26	11.6 ± 1.8	18.6 ± 3.3
[^{18}F]FEDPN[b]	1.67 ± 0.29	1.46 ± 0.32	1.29 ± 1.03	1.32 ± 0.25	0.79 ± 0.13	0.61 ± 0.28
[^{18}F]FES/[^{18}F]FEDPN	2.08	8.22	19.7	1.97	14.7	30.5

[a] αERKO mice were in diestrus but βERKO mice were in estrus. [b] All mice were in diestrus. [c] The ratios of βERKO/αERKO of [^{18}F]FES and [^{18}F]FEDPN in uterus and ovaries are expressed as the mean ± SD.

targeting. The ERβ gene remains functional in these animals;[40] however, female αERKO mice have hypoplastic uteri and hyperemic ovaries with no apparent corpora lutea, and they are infertile.[40] Later, the ERβ knock-out (βERKO) mouse model was generated using a similar gene targeting method. The ERα gene remains functional in these animals,[41] and the uteri of female βERKO mice appear to be anatomically normal compared to αERKO.[42]

In analyses below, we have frequently used as a measure of the ER subtype selectivity of the uptake, the ratio of uptake of a compound in the two ER knockout animal models: When the αERKO/βERKO ratio >1, it highlights preferential interaction with ERβ (because the αERKO animals contain only ERβ, whereas the βERKO animals contain only ERα); by contrast, when the inverse ratio βERKO/αERKO >1, it highlights preferential interaction with ERα.

Tissue Distribution of [^{18}F]FES in ERKO Mice. As a first step, we used [^{18}F]FES to see how alteration of the levels of the ER subtypes in these knockout mice would affect in vivo uptake of an ER ligand whose distribution pattern in other species, including humans, had been well characterized.[38,43−46] As expected from its 6.3-fold ERα absolute affinity selectivity, [^{18}F]FES uptake in βERKO animals was higher than that in αERKO mice in all selected organs (Table 4). The highest %ID/g was observed in the uterus of diestrus βERKO mice at 30 min postinjection (18.9 ± 0.1%ID/g).

As described in the Experimental Section in detail, only two βERKO mice were in diestrus for the biodistribution study at 30 min postinjection. All other biodistribution studies with βERKO mice were done during estrus because of experimental complications, primarily false pregnancy presumably induced by repeated swab testing. For all organs except the uterus, uptake of [^{18}F]-FES was similar at 30 min in both estrus and diestrus

βERKO mice. The %ID/g in the uterus of βERKO mice during estrus was roughly half that of during diestrus, though still very high (8.34 ± 2.91 vs 18.9 ± 0.1). This is similar to our earlier studies of the effect of estrus on radioestrogen biodistribution in rats.[47] In case of 16α-[^{125}I]iodoestradiol, uterus/blood and uterus/nontarget ratios at 1 h postinjection were about 3-times higher during diestrus than during estrus.[47]

All biodistribution studies in αERKO mice, which lack the ERα subtype to which FES binds preferentially, were done in diestrus. Thus, not surprisingly, because they lack ERα, uterine uptake in αERKO mice at 30 min is 7.9-fold lower than that in βERKO mice in diestrus (2.40 ± 0.49 vs 18.9 ± 0.1). While the uterine uptake of [^{18}F]FES in βERKO mice in estrus was high and increased at 1 h (8.3 at 30 min; 9.8 at 1 h), that in αERKO mice was lower, peaking at 30 min and washing out by 2 h.

The βERKO/αERKO ratio of uterine uptake of [^{18}F]-FES increased from 3.5 ± 0.6 at 30 min to 12.0 ± 1.4 at 1 h and 25.4 ± 1.8 at 2 h, consistent with ERα being the dominant factor determining [^{18}F]FES uptake in this organ (Table 5). Similarly, ovary uptake of [^{18}F]-FES in βERKO mice (in estrus) peaked at 30 min (6.5 ± 0.6%ID/g) and then slowly decreased (5.6 ± 1.3 at 1 h; 3.4 ± 0.8 at 2 h), whereas in αERKO mice, ovary uptake rapidly decreased, resulting in a higher βERKO/αERKO ratio at later time points (2.6 ± 0.3 at 30 min; 11.6 ± 1.8 at 1 h; 18.6 ± 3.3 at 2 h).

Interestingly, there was no significant difference in ovary uptake of [^{18}F]FES in estrus and diestrus βERKO mice (6.5 ± 0.6 vs 6.6 ± 2.7%ID/g). All other organs but one also showed comparable activity uptake both in diestrus and in estrus; only uterus uptake of [^{18}F]FES seemed to be highly dependent on the stage of the estrous cycle. The strong dependence of uterus uptake on estrous cycling could be attributed to variations in endogenous ER ligand concentrations, mostly estradiol.

Table 6. Serum Estradiol Levels in BALB/c in Diestrus and βERKO in Estrus

mouse	concentrated of estradiol[a] (pg/mL)
BALB/c (diestrus)	28.7 ± 5.7
βERKO (estrus)	43.8 ± 3.1

[a] Values are reported as the mean ± SD with three samples per mouse.

We measured the circulating level of estradiol in the serum of control BALC/c mice and βERKO mice in estrus (Table 6, $n = 3$ each). Serum was collected from all mice, and samples were sent to an outside laboratory (AniLytics, Inc., Gaithersburg, MD) for determination of estradiol (E2) levels. 17β-Estradiol is not a species specific hormone; therefore, the radioimmunoassay was performed using commercially available reagents for testing human serum (MP Biomedicals). As the assay is run, both free and protein-bound estradiol are measured in each serum sample.

Estradiol levels in βERKO mice in estrus were 1.5 times higher than in BALB/c mice in diestrus (43.8 vs 28.7 pg/mL). The estradiol level in BALB/c mice (28.7 pg/mL) is comparable with that of αERKO mice (29.5 pg/mL) and that of βERKO mice (30.5 pg/mL).[48,49] The serum estradiol level of βERKO mice in estrus was much higher than the reported value in adult βERKO females (43.8 vs 24.2 pg/mL).[48] Higher endogenous estradiol levels during estrus might effectively block the limited number of ER binding sites in uterus, accounting for decreases in uterine uptake during estrus compared to during nonestrus.

In organs other than uterus, ovaries and liver, the highest βERKO/αERKO uptake ratio of [18F]FES was at 1 h postinjection. In the cases of muscle and fat, these ratios were above 7.2 at 1 h and 4.8 at 2 h. Spleen, brain, bone, and thymus also showed βERKO/αERKO ratio of greater than 4 at 1 h. These sizable ratios for nominally estrogen nontarget tissues might reflect the fact that they contain small, but significant amounts of ER, as do, in fact, most tissues.[12,48] Blood, liver, and kidney uptakes in βERKO mice, however, were slightly higher than corresponding values in αERKO mice at all time points. Compared to biodistribution of [18F]FES in immature female Sprague−Dawley rats,[44] both sets of ERKO mice showed higher blood retention at all time points, but faster clearance through liver and kidney.

Tissue Distribution of [18F]FEDPN in ERKO Mice. Comparisons of organ uptake of [18F]FEDPN in

αERKO and βERKO mice are summarized in Table 7. FEDPN has a RBA of 8.7 with ERβ and 0.42 with ERα subtype, giving it an ERβ selectivity of 21 based on RBA values and an 8.3-fold ERβ selectivity based on absolute affinities (Table 2). Even though the RBA of FEDPN for ERβ is less than 10% of that of estradiol, because of its greatly reduced binding affinity for ERα (less than 0.5% than estradiol), different tissue distribution patterns are expected in αERKO versus βERKO mice.

In contrast to the ERα-preferential ligand [18F]FES, with which all uptake levels in βERKO mice were higher than those in αERKO mice, many organs showed higher uptake of [18F]FEDPN in αERKO rather than βERKO mice, particularly at later time points, consistent with the presence of ERβ in the αERKO animals and the preferential affinity of [18F]FEDPN for ERβ. At 2 h postinjection, all organs except liver, brain, and uterus showed higher uptake in αERKO mice compared to corresponding values in βERKO. However, the αERKO/βERKO uptake ratio was less than 2 in most organs except thymus, which could be attributed to the relatively low binding affinities of FEDPN for both ER subtypes.

The most striking difference in organ uptake between [18F]FES and [18F]FEDPN was found in uterus. In case of [18F]FES, the uterine βERKO/αERKO uptake ratio increased from 3.5 ± 0.6 at 30 min to 12.0 ± 1.4 at 1 h and 25.4 ± 1.8 at 2 h, even though the βERKO mice were in estrus. Considering that uterine uptake of [18F]-FES in βERKO mice during diestrus is more than twice that during estrus (18.9 vs 8.3%ID/g), the uterine βERKO/αERKO uptake ratio in uterus might also be doubled during diestrus. By contrast, the βERKO/αERKO uterine uptake ratio of [18F]FEDPN was always less than 2, and furthermore the ratio was decreased over time from 1.7 ± 0.3 at 30 min to 1.5 ± 0.3 at 1 h and then 1.3 ± 1.0 at 2 h (Table 5). Compared to those of [18F]FES, these uptake ratios for [18F]FEDPN are consistent with what is expected for this ERβ-selective ligand, although the level of preferential uptake is quite modest, reflecting the lower affinity of [18F]FEDPN for ERβ.

When the biodistribution of [18F]FEDPN in immature female Sprague−Dawley rats (Table 3) is compared with that in both sets of ERKO mice (Table 7), similar activity uptake and clearance patterns are found.

Comparison of βERKO/αERKO Uterine and Ovary Uptake Ratio of [18F]FES and [18F]FEDPN.

Table 7. Biodistribution of [18F]FEDPN in αERKO and βERKO Mice[a]

organ	αERKO			βERKO		
	30 min	1 h	2 h	30 min	1 h	2 h
blood	0.73 ± 0.15	0.42 ± 0.11	0.23 ± 0.01	0.79 ± 0.02	1.12 ± 1.14	0.18 ± 0.04
lung	4.32 ± 0.80	2.04 ± 0.72	0.75 ± 0.28	5.38 ± 0.36	1.71 ± 0.33	0.44 ± 0.08
liver	3.70 ± 0.73	3.80 ± 2.26	1.93 ± 0.19	4.55 ± 0.68	3.79 ± 2.74	2.04 ± 0.56
spleen	0.99 ± 0.32	0.61 ± 0.68	0.12 ± 0.02	0.87 ± 0.17	0.40 ± 0.23	0.12 ± 0.05
kidney	7.22 ± 2.97	2.97 ± 0.83	1.94 ± 0.86	4.83 ± 0.54	2.42 ± 1.33	1.39 ± 0.12
muscle	1.21 ± 0.26	0.59 ± 0.39	0.36 ± 0.35	1.45 ± 0.37	0.75 ± 0.50	0.27 ± 0.23
fat	0.57 ± 0.08	0.27 ± 0.17	0.09 ± 0.01	0.89 ± 0.42	0.33 ± 0.16	0.09 ± 0.06
heart	1.57 ± 0.38	0.74 ± 0.41	0.25 ± 0.02	1.60 ± 0.05	0.43 ± 0.03	0.21 ± 0.03
brain	0.96 ± 0.11	0.51 ± 0.08	0.28 ± 0.05	0.93 ± 0.16	0.47 ± 0.04	0.30 ± 0.08
bone	3.47 ± 0.50	4.13 ± 0.95	5.45 ± 1.86	3.35 ± 0.69	4.92 ± 0.77	5.15 ± 0.43
uterus	1.11 ± 0.50	0.37 ± 0.21	0.24 ± 0.11	1.85 ± 0.15	0.54 ± 0.13	0.31 ± 0.19
ovaries	1.06 ± 0.09	0.52 ± 0.10	0.28 ± 0.04	1.40 ± 0.54	0.41 ± 0.14	0.17 ± 0.09
thymus	1.27 ± 0.52	0.68 ± 0.51	0.28 ± 0.08	1.20 ± 0.03	0.25 ± 0.07	0.11 ± 0.04

[a] Data are expressed as the %ID/g SD with three animals per data point.

Overall, there is a very clear distinction between the pattern, level, and time course of tissue uptake of the two radiolabeled compounds that seems to be consistent with their different binding preferences for the two ER subtypes. If our animal models were hypothesized to reflect these in vitro binding affinities precisely, then the βERKO/αERKO ratio of [18F]FES in uterus should be 52 times (6.3 × 8.3) higher than that of [18F]FEDPN. Actually, the βERKO/αERKO ratio of [18F]FES uptake in the uterus at 2 h was calculated to be 20 times higher than that of [18F]FEDPN (25.4 vs 1.3) (Table 5). In addition, considering, as we noted above, that this uptake ratio might more than double in animals during diestrus compared with those in estrus, the number, 46 (20 × 2.3), would actually be even closer to the theoretical value, 53.

We hasten to note that this simple calculation is made for illustrative purposes only, and one should not anticipate being able to predict the βERKO/αERKO uterine uptake ratio based solely on in vitro binding affinity results, because this does not take into consideration many important physiological factors, including the different anatomy and histology of αERKO and βERKO animals, the different endogenous hormone levels in the two ERKO mice, and different patterns of ER expression in tissue. For example, reproductive tract in βERKO mice is normal, whereas the uteri in αERKO mice are underdeveloped and the ovaries are enlarged due to hemorrhagic cysts.[50] Furthermore, αERKO female mice have elevated estradiol and testosterone levels, whereas the βERKO ovaries produce normal serum levels of estradiol and testosterone.[48,50] Also, Korach et al. recently reported that ERβ mRNA is barely detectable in the rodent uterus, including those from αERKO mice.[48,51,52] In our biodistribution study with [18F]FES, the uptake ratios of uterus-to-blood and uterus-to-muscle were over 3 in αERKO mice at all time points, indicating that this ligand can show ERβ receptor-mediated selective uptake in the uterus, even though the level of ERβ protein in the uterus is low and the receptor binding is likely blocked, at least to some extent, by high endogenous estradiol levels.[52] Interestingly, uterine uptake of [18F]FES in αERKO mice was about double that of [18F]FEDPN at all time points, which is comparable with the 2.5-fold higher RBA of [18F]FES for ERβ compared to that of [18F]FEDPN (22.0 vs 8.7; Table 2). The fact that [18F]FES is ERα preferential is irrelevant in animals in which this ER subtype has been knocked out.

In contrast to the uterus, both ERα and ERβ are clearly expressed in ovary in rodents.[12,48] Highest expression of ERβ mRNA was observed in the ovary and prostate of rats.[12] Therefore, the uptake ratio in ovaries between two knockout models might reflect ligand binding selectivity better than that in uterus. Even though the αERKO/βERKO uptake ratios of [18F]-FEDPN in uterus were less than 0.8 at all three time points and remained relatively constant, *ovary* uptake ratios of αERKO/βERKO increased over time from 0.8 at 30 min to 1.3 at 1 h and then 1.6 at 2 h (Table 5), consistent with ERβ-dominated uptake in this organ. By comparison, the ovarian βERKO/αERKO uptake ratio for [18F]FES was 30 at 2 h postinjection, which is slightly lower than 46 in uterus and 52 from the in vitro RBA-based calculation.

Discussion

In this study, we have sought to develop a fluorine-18-labeled radioligand that would be effective in imaging ERβ by PET. Thus, we have synthesized and examined the tissue distribution of an ERβ-selective ligand, [18F]FEDPN, in various animal models, in some cases comparing this distribution with that of [18F]FES, a well-studied radiopharmaceutical for imaging ER. The unlabeled standard of FEDPN and its precursor were synthesized by using benzyl and MEM groups to protect the phenols, respectively, and [18F]FEDPN was successfully labeled with [18F]fluoride ion in high specific activity. FEDPN has moderate in vitro ERβ binding selectivity, but its absolute binding affinity values are considerably lower than those of the non-fluorine substituted analogues of DPN. In immature female Sprague−Dawley rats there was weak but meaningful specific uptake of FEDPN in the uterus and ovaries that was blocked by coadministration with estradiol.

αERKO and βERKO mice were found to be good animal models to assess the ER subtype selectivity of radioligand uptake in target tissues. [18F]FES, which has a higher affinity for both of the ER subtypes and a 6.3-fold preference for ERα, showed very high βERKO/αERKO uptake ratios for uterus and ovaries at 2 h (25.4 and 18.6, respectively), clear evidence for the involvement of ERα. By contrast, the uterine βERKO/αERKO uptake ratios with [18F]FEDPN was always less than 2 and decreased over time, wherease the ovary αERKO/βERKO uptake ratios with [18F]FEDPN increased over time, reaching a maximum of 1.6 at 2 h. While the uptake preferences of [18F]FEDPN are not sufficiently pronounced to be useful for PET imaging of ERβ, they suggest that the distribution of [18F]FEDPN is being regulated by an ERβ-mediated process. A strong dependence of uterus uptake of [18F]FES upon estrus cycle in mice has also been demonstrated. Thus, overall, the time course and target tissue distribution patterns of both [18F]FES and [18F]FEDPN in the two ERKO mice systems are consistent with their absolute and preferential affinities for ERα and ERβ, respectively, as well as the relative levels of these two ER subtypes in the ERKO animals.

From this work, we can make a number of other conclusions: Even though its ERα absolute binding selectivity is only 6.3, [18F]FES is a very effective agent for imaging ERα; its affinity for this ER subtype is very high, and in most tissues, ERα is by far the predominant ER. Still, it might be possible to improve the selectivity of ERα imaging by using some FES analogues that have a somewhat greater ERα binding preference. For example, while the closest FES analogue, 17β-ethynyl-FES,[53] has a similar ERα/ERβ absolute binding selectivity ratio of 6.0, another 17-ethynyl-substituted FES compound, 17α-ethynyl-FES (FEES),[53] has somewhat higher ERα absolute selectivity (ERα/ERβ 11).[54]

Even though [18F]FEDPN, the principal subject of this study, showed some significant binding selectivity for the ERβ subtype in in vivo animal studies, its absolute

binding affinity for the estrogen receptors is not high enough for it to be effective in imaging studies. Therefore, radioligands with higher affinity and greater selectivity for ERβ are needed. In this regard, it is of note that Malamas and co-workers have recently reported new diphenolic azoles as highly selective ERβ agonists.[55] The more potent and selective analogues of these series have binding affinities for ERβ that are comparable to that of the natural ligand 17β-estradiol, yet are >100-fold selective over ERα. The 7-position-substituted benzoxazoles were the most selective ligands of both azole series, with ERB-041 being >200-fold selective for ERβ. ER ligands based on this compound series might prove to be effective agents for imaging ERβ in vivo. Compounds with comparable ERβ affinity and selectivity in the indazole system were also reported by us recently.[56]

While we have used the ERα and ERβ knockout mice in a relatively straightforward manner to help us characterize the respective roles of the ERβ and ERα subtypes in the uptake process of the ^{18}F-ligands, it is of note that more sophisticated experimental designs should also be considered. In our biodistribution studies, the animals were not ovariectomized, because the ovaries were used as critical target organs. These are adult animals, however, and as we have noted, their high levels of circulating estradiol are likely to compete for receptor binding with the ^{18}F-ligands. While an uptake blocking study using estradiol as a blocking agent might be informative in this respect, an improved experimental design, suggested by a reviewer, might be to pretreat the animals with an aromatase inhibitor such as letrozole, or a steroidogenic inhibitor such as aminoglutethimide. In this way, circulating levels of estradiol could be lowered without removing the ovaries. An alternative model for ERβ uptake might be the prostate of the castrated male rat, which is relatively rich in ERβ; circulating estradiol levels are also low. These alterative in protocols, as well as the use of ER-subtype selective ligands in blocking the uptake of estrogen radiotracers in wild-type animals will be considered in our future studies.

Experimental Section

General Methods and Materials. 4-(Benzyloxy)phenylacetonitrile was purchased from Oakwood Products, Inc (West Columbia, SC) and all other solvents and reagents were obtained from Aldrich and used as received without any further purification. An unlabeled standard for 16α-[^{18}F]-fluoroestradiol-17β was purchased from ABX advanced biochemical compounds (Radeberg, Germany). Water was distilled and then deionized (18 MΩ/cm²) by passing through a Milli-Q water filtration system (Millipore Corp., Bedford, MA). ^{1}H and ^{13}C NMR spectra were measured using a Varian Gemini 300 instrument, and chemical shifts are reported in ppm on the δ scale relative to TMS or solvent peak. Proton chemical shifts are annotated as follows: ppm (multiplicity, coupling constant (Hz), integral). Mass spectra were obtained from Washington University Mass Spectrometry Resource.

H_2^{18}O was purchased from Rotem Industries (Israel). ^{18}F-Fluoride was produced in Washington University by the ^{18}O-(p,n)^{18}F reaction through proton irradiation of enriched (95%) ^{18}O water using either the JSW BC16/8 cyclotron (The Japan Steel Works Ltd, Tokyo, Japan) or the CS15 cyclotron (The Cyclotron Corp., Berkeley, CA). Materials were heated using a custom-designed microwave cavity, model 420BX (Micro-Now Instruments, Skokie, IL).[57] Screw-cap test tubes used for microwave heating were purchased from Fisher Scientific (Pyrex No. 9825). Oasis cartridges were purchased from Waters Corporation, (HLB-6 cc, Part No.186000115). For the TLC analyses, EM Science Silica Gel 60 F$_{254}$ TLC plates were purchased from Fisher Scientific (Pittsburgh, PA). Radio-TLC was accomplished using a Bioscan 200 imaging scanner (Bioscan, Inc., Washington, DC). Radioactivity was counted with a Beckman Gamma 8000 counter containing a NaI crystal (Beckman Instruments, Inc., Irvine, CA). High performance liquid chromatography (HPLC) was performed with a SpectraSYSTEM P2000 liquid chromatography, equipped with an ultraviolet detector operating at 254 nm and a well−scintillation NaI (Tl) detector and associated electronics, and a fraction collector.

The purification of the final product was achieved using a semipreparative HPLC Chromanetics C18 column (Partisil ODS-3, 100×10 mm, 5 μm, MeCN:EtOH:H$_2$O (2:20:78), 3 mL/min). For the quality control, the radiochemical purity of the [^{18}F]FEDPN was assayed by analytical radioHPLC (Alltech, Econosil C18 column, 250 × 4.6 mm, 10 μm; 0.1 M formate: MeCN (60:40) at a flow rate of 1.5 mL/min and UV at 254 nm) in the presence of the unlabeled compound as standard. TLC was used in determining the compounds during various synthesis steps (silica, ethyl acetate:hexane = 3:1 v/v). Radiochemical yields are decay corrected to the beginning of synthesis time (BOS).

Immature female Sprague−Dawley rats were purchased from Charles River Laboratories, and αERKO and βERKO mice were obtained from Taconic Inc. (Germantown, NY). Estrogen receptor knockout mice (α/βERKO) were staged according to the estrous cycle by microscopic examination of daily prepared vaginal smears[47] and were subjected to biodistribution study during diestrus. The circulating estradiol level in serum was measured in Ani Lytics, Inc. (Gaithersburg, MD). All animal experiments were conducted in compliance with the Guidelines for the Care and Use of Research Animals established by Washington University's Animal Studies Committee.

Cold Synthesis. (Z)-2,3-Bis(4-methoxyphenyl)acrylonitrile (**1a**) was prepared by a modification of a previously described method.[21]

(2R*,3S*)-2,3-Bis(4-methoxyphenyl)pent-4-enenitrile (2a). To a mixture of (Z)-2,3-bis(4-methoxyphenyl)acrylonitrile (2770 mg, 10.4 mmol) and CuI (198 mg, 1.04 mmol) in dried THF (30 mL) was added 1 M vinylmagnesium bromide (21 mL) dropwise at −76 °C. The flask was allowed to warm to room-temperature overnight with stirring under Ar atmosphere. The mixture was quenched by saturated NH$_4$Cl solution. After filtering off the precipitate, the filtrate was diluted with 40 mL of CH$_2$Cl$_2$, washed by brine, dried over Na$_2$SO$_4$, and concentrated under vacuum. The residue was recrystallized for 1 h from refluxing ethyl acetate/hexane (1:1) to give white solid (erythro:threo = 9:1). Repeated recrystallization from refluxing ethyl acetate/hexane (1:1) gave pure *erythro*−**2a**. (1671 mg, 55%): ^{1}H NMR (CDCl$_3$, 300 MHz) δ 3.58 (t, J = 8.0 Hz, 1H), 3.68 (s, 6H), 3.94 (d, J = 9.0 Hz, 1H), 5.12 (m, 2H), 6.14 (m, 1H), 6.74 (m, 4H), 6.99 (m, 4H); ^{13}C NMR (CDCl$_3$, 75 MHz) δ 43.5 (*C*HCN), 53.9 (*C*HCH=CH$_2$), 55.39 and 55.45 (O*C*H$_3$), 114.1 and 114.2 (Ph ring *C*H), 117.9 (CHCH=*C*H$_2$), 120.1 (*C*N), 126.0, 129.1 and 129.4 (Ph ring *C*H), 130.9, 137.1 (*C*HCH=*C*H$_2$), 159.1 and 159.5 (Ph ring *C*). HRMS (FAB): *m/z* 300.1566 ([M + Li]$^+$, C$_{19}$H$_{19}$NO$_2$Li, calcd 300.1576).

(2R*,3S*)-5-Hydroxy-2,3-bis(4-methoxyphenyl)pentanenitrile (3a). To a clear THF solution (15 mL) of (2R*,3S*)-2,3-bis(4-methoxyphenyl)pent-4-enenitrile (439 mg, 1.50 mmol) was added 1 M BH$_3$·THF (1.7 mL) dropwise at −40 °C. The mixture was allowed to warm to room temperature over 1 h and was kept stirring for an additional 1.5 h under an Ar atmosphere. After quenching excess BH$_3$ with water (2 mL), 0.5 M NaOH (3 mL) and 35% H$_2$O$_2$ (300 μL) were added to the mixture at 0 °C. The flask was stirred for 1 h at 0 °C. The mixture was diluted with water (20 mL), then extracted by ethyl acetate (20 mL). After layer separation, the aqueous layer was further extracted by same amount of ethyl acetate. The

combined organic layers were washed by $NaHCO_3$ and brine, dried over Na_2SO_4, and concentrated to give clear oil. The crude product was chromatographed over silica using ether as eluent to give white solid. (313 mg, 67%): ^{1}H NMR (CDCl$_3$, 300 MHz) δ 1.99 (m, 2H), 3.15 (m, 1H), 3.34−3.58 (m, 2H), 3.758 (s, 3H), 3.761 (s, 3H), 4.01 (d, J = 6.3 Hz, 1H), 6.79 (m, 4H), 6.98 (m, 4H); ^{13}C NMR (CDCl$_3$, 75 MHz) δ 35.8 (CCH$_2$-CH$_2$OH), 43.8 (CCN), 46.4 (CCH$_2$CH$_2$OH), 55.2 and 55.3 (OCH$_3$), 60.1 (CH$_2$$CH_2$OH), 113.9 and 114.1 (Ph ring CH), 120.2 (CN), 126.4, 129.4 and 129.6 (Ph ring CH), 130.7, 159.0 and 159.3 (Ph ring C). HRMS (FAB): m/z 318.1688 ([M + Li]$^+$, $C_{19}H_{21}NO_3Li$, calcd 318.1681).

(2R^*,3S^*)-5-Fluoro-2,3-bis(4-methoxyphenyl)pentane-nitrile (4a). To a dry CH$_2$Cl$_2$ solution (8 mL) of (2R^*,3S^*)-5-hydroxy-2,3-bis(4-methoxyphenyl)pentanenitrile (285 mg, 0.92 mmol) was added (diethylamino)sulfur trifluoride (DAST, 600 μL, 4.58 mmol) dropwise at −76 °C. The mixture was stirred under Ar atmosphere and allowed to warm to room-temperature overnight. After quenching with saturated NaHCO$_3$ at 0 °C, the solution was diluted with water (15 mL), then extracted CH$_2$Cl$_2$ (2 × 15 mL), dried over MgSO$_4$, and concentrated in vacuo. The crude product was purified by flash chromatography (silica, ethyl acetate/hexane (1:1)) to give a pale yellow solid. (187 mg, 65%): ^{1}H NMR (CDCl$_3$, 300 MHz) δ 1.98−2.32 (m, 2H), 3.19 (m, 1H), 3.80 (s, 6H), 4.02 (d, J = 6.9 Hz, 1H), 4.10−5.31 (m, 2H), 6.20 (m, 4H), 7.01 (m, 4H); ^{13}C NMR (CDCl$_3$, 75 MHz) δ 34.1 (d, J_{CF} = 20.0 Hz, CH$_2$CH$_2$F), 43.8 (CHCN), 46.1 (d, J_{CF} = 4.1 Hz, CHCH$_2$CH$_2$F), 55.40 and 55.49 (OCH$_3$), 81.6 (d, J_{CF} = 164.7 Hz, CH$_2$$CH_2$F), 114.2 and 114.3 (Ph ring CH), 120.0 (CN), 126.2, 129.5 and 129.7 (Ph ring CH), 130.0, 159.3, 159.6. HRMS (FAB): m/z 320.1635 ([M + Li]$^+$, $C_{19}H_{20}FNO_2Li$, calcd 320.1638).

(Z)-2,3-Bis(4-(benzyloxy)phenyl)acrylonitrile (1b). The mixture of 4-(benzyloxy)benzaldehyde (5257 mg, 24.8 mmol), 4-(benzyloxy)phenylacetonitrile (5530 mg, 24.8 mmol), and NaOMe (156 mg, 2.89 mmol) in dry ethanol (100 mL) was refluxed for 2 h and cooled to room temperature to produce a precipitate of white crystals. After removing the solid by filtration, to the filtrate was added more NaOMe (503 mg, 9.31 mmol), and the mixture was refluxed for 2 h and cooled to room temperature to precipitate more crystals. After second crop, the filtrate was concentrated and the residue was redissolved in CH$_2$Cl$_2$, washed by brine, dried over MgSO$_4$, and concentrated. The residue was dissolved in EtOH (80 mL) again, then NaOMe (579 mg, 10.7 mmol) was added. The mixture was refluxed for 3 h, then cooled to room temperature to give white crystals. All crops were washed with a small amount of ethanol and dried in air. (10.02 g, 97%): ^{1}H NMR (CDCl$_3$, 300 MHz) δ 5.12 (s, 2H), 5.14 (s, 2H), 7.04 (m, 4H), 7.36 (s, 1H), 7.44 (m, 10H), 7.59 (m, 2H), 7.86 (m, 2H); ^{13}C NMR (CDCl$_3$, 75 MHz) δ 70.4 (OCH$_2$Ph), 108.7 (CH=CCN), 115.4 and 115.5 (Ph ring CH), 118.8 (CN), 127.2, 127.3, 127.7, 128.35, 128.41, 128.9, 131.1, 136.6, 136.7, 140.2 (CH=CCN), 159.5, 160.6. HRMS (FAB): m/z 417.1726 ([M]$^+$, $C_{29}H_{23}NO_2$, calcd 417.1729).

(2R^*,3S^*)-2,3-Bis(4-(benzyloxy)phenyl)pent-4-enenitrile (2b). To a dry THF solution (35 mL) of (Z)-2,3-bis(4-(benzyloxy)phenyl)acrylonitrile (3433 mg, 8.22 mmol) and CuI (157 mg, 0.82 mmol) was added 1 M vinylmagnesium bromide (10 mL) dropwise at −25 °C. The flask was allowed to warm to room temperature over 1 h and stirred overnight under Ar gas atmosphere. The reaction was quenched by saturated NH$_4$Cl, and the mixture was stirred for 2 h at 0 °C. After filtering off the precipitate, the filtrate was concentrated, redissolved in ethyl acetate, then washed by NaHCO$_3$ solution, dried over MgSO$_4$, and concentrated. The crude product was recrystallized for 1 h from refluxing ethanol to give a white solid. Repeated recrystallization from refluxing ethanol gave pure *erythro*−2b (1695 mg, 46%): ^{1}H NMR (CDCl$_3$, 300 MHz) δ 3.64 (t, J = 7.7 Hz, 1H), 3.99 (d, J = 7.2 Hz, 1H), 5.04 (s, 4H), 5.12 (d, J = 17 Hz, 1H), 5.26 (d, J = 10 Hz, 1H), 6.20 (m, 1H), 6.89 (m, 4H), 7.05 (m, 4H), 7.37 (m, 10H); ^{13}C NMR (CDCl$_3$, 75 MHz) δ 43.9 (CHCN), 54.6 (CHCH=CH$_2$), 70.2 (OCH$_2$Ph), 115.15 and 115.19 (Ph ring CH), 118.9 (CHCH=CH$_2$), 120.2 (CN), 126.6, 127.7, 128.20, 128.26, 128.8, 129.2, 129.5, 132.0,

136.3 (CHCH=CH$_2$), 136.9 and 137.1 (OCH$_2$$C$), 158.2 and 158.6 ($COCH_2$). HRMS (FAB): m/z 452.2184 ([M + Li]$^+$, $C_{31}H_{27}NO_2Li$, calcd 452.2202).

(2R^*,3S^*)-2,3-Bis(4-(benzyloxy)phenyl)-5-hydroxypen-tanenitrile (3b). To a dry THF solution (20 mL) of (2R^*,3S^*)-2,3-bis(4-(benzyloxy)phenyl)pent-4-enenitrile (503 mg, 1.13 mmol) was added 1 M BH$_3$·THF (1.6 mL) dropwise at 0 °C. The flask was allowed to warm to room temperature slowly and stirred for 5 h under Ar gas atmosphere. The mixture was cooled to 0 °C again and quenched by water (2 mL). 3 M NaOH (4 mL) and 35% H$_2$O$_2$ (4 mL) were added, and the resulting reaction mixture was stirred for 30 min more in ice bath. The solution was diluted with water (15 mL) and extracted by ethyl acetate (2 × 20 mL). The combined organic layer was washed by saline, dried over MgSO$_4$, and concentrated. The crude product was chromatographed over silica using ethyl acetate/hexane (1:1) to give pure product. (228 mg, 44%): ^{1}H NMR (CDCl$_3$, 300 MHz) δ 2.02−2.26 (m, 2H), 3.19−3.41 (m, 2H), 3.56 (m, 1H), 3.95 (d, J = 7.2 Hz, 1H), 5.040 (s, 2H), 5.044 (s, 2H), 6.91 (m, 4H), 7.07 (m, 4H), 7.42 (m, 10H); ^{13}C NMR (CDCl$_3$, 75 MHz) δ 34.6 (CHCH$_2$CH$_2$OH), 44.2 (CHCN), 46.6 (CH$_2$CH$_2$OH), 60.2 (CH$_2$$CH_2$OH), 70.1 (O$CH_2$Ph), 115.1 (Ph ring CH), 120.4 (CN), 126.6, 127.6, 128.08 and 128.14 (Ph ring CH), 128.7, 129.35 and 129.40 (Ph ring CH), 131.5, 136.8 and 137.0 (OCH$_2$$C$), 158.2 and 158.5.

(2R^*,3S^*)-2,3-Bis(4-(benzyloxy)phenyl)-5-fluoropen-tanenitrile (4b). To a solution of (2R^*,3S^*)-2,3-bis(4-(benzyloxy)phenyl)-5-hydroxypentanenitrile (157 mg, 0.34 mmol) in dry CH$_2$Cl$_2$ (6 mL) was added (diethylamino)sulfur trifluoride (DAST, 222 μL, 1.69 mmol) dropwise at −76 °C. The mixture was stirred under Ar gas and allowed to warm to room-temperature overnight. The flask was cooled to 0 °C again and quenched by saturated NaHCO$_3$. The solution was diluted by water (15 mL), then extracted by CH$_2$Cl$_2$, dried over MgSO$_4$, and concentrated. The crude product was recrystallized in refluxing ethanol to give pale yellow crystal. (83 mg, 53%): ^{1}H NMR (CDCl$_3$, 300 MHz) δ 2.02−2.50 (m, 2H), 3.24 (m, 1H), 3.97 (d, J = 6.6 Hz, 1H), 4.06−4.51 (m, 2H), 5.06 (s, 4H), 6.93 (m, 4H), 7.09 (m, 4H), 7.42 (m, 10H); ^{13}C NMR (CDCl$_3$, 75 MHz) δ 32.5 (d, J_{CF} = 20.5 Hz, CH$_2$CH$_2$F), 44.1 (CHCN), 46.1 (d, J_{CF} = 4.5 Hz, CHCH$_2$CH$_2$F), 70.2 (OCH$_2$Ph), 81.4 (d, J_{CF} = 165.1 Hz, CH$_2$$CH_2$F), 115.3 (Ph ring CH), 120.1 (CN), 126.4, 127.6, 128.17, 128.22, 128.7, 129.4, 130.9, 136.8 and 137.0 (OCH$_2$$C$), 158.4 and 158.7 ($COCH_2$).

(2R^*,3S^*)-5-Fluoro-2,3-bis(4-hydroxyphenyl)pentane-nitrile (5). To a clearly dissolved solution of (2R^*,3S^*)-2,3-bis(4-(benzyloxy)phenyl)-5−fluoropentanenitrile (83 mg, 0.18 mmol) in ethyl acetate (15 mL) was added 10% Pd/C (106 mg), and the mixture was stirred under H$_2$ gas for 4 h. The Pd/C catalyst was filtered off through a Celite plug and washed with small amount of ethyl acetate and MeCN. After concentration, the residue was purified by flash chromatography (silica, ethyl acetate/hexane (1:1)) to give a clear oil. (39 mg, 77%): ^{1}H NMR (acetone-d_6, 300 MHz) δ 2.04−2.48 (m, 2H), 3.22 (m, 1H), 4.04−4.48 (m, 2H), 4.19 (d, J = 8.1 Hz, 1H), 6.75 (m, 4H), 7.04 (m, 4H), 8.41 (b s, 2H); ^{13}C NMR (acetone-d_6, 75 MHz) δ 34.0 (d, J_{CF} = 19.4 Hz, CH$_2$CH$_2$F), 44.0 (CCN), 46.6 (d, J_{CF} = 5.7 Hz, CCH$_2$CH$_2$F), 82.3 (d, J_{CF} = 162.8 Hz, CH$_2$$CH_2$F), 116.2 and 116.3 (Ph ring CH), 121.4 (CN), 126.7, 130.4 (Ph ring CH), 130.6, 157.5 and 158.0 (Ph ring C). HRMS (ESI): m/z 286.1232 ([M + H]$^+$, $C_{17}H_{17}FNO_2$, calcd 286.1243). R_f = 0.58 (silica, ethyl acetate:hexane = 3:1).

(2R^*,3S^*)-2,3-Bis(4-hydroxyphenyl)pent-4-enenitrile (6). To a solution of (2R^*,3S^*)-2,3-bis(4-methoxyphenyl)pent-4-enenitrile (473 mg, 1.61 mmol) in anhydrous CH$_2$Cl$_2$ was added 1 M BBr$_3$ (7 mL) in portions at 0 °C. The solution was allowed to warm to room temperature slowly and stirred overnight. The reaction was quenched by water (2 mL) at 0 °C. The mixture was diluted by ethyl acetate (30 mL), then washed by brine solution, dried over MgSO$_4$, and concentrated completely under vacuum to give a pale yellow solid. (422 mg, 99%): ^{1}H NMR (acetone−d_3, 300 MHz) δ 3.76 (t, J = 8.3 Hz, 1H), 4.33 (d, J = 8.4 Hz, 1H), 4.98 (m, 2H), 6.01 (m, 1H), 6.80 (m, 4H), 7.11 (m, 4H), 8.30 (s, 1H), 8.46 (s, 1H); ^{13}C NMR

(acetone−d₃, 75 MHz) δ 43.3 (*C*HCN), 54.8 (*C*HCH=CH₂), 116.15 and 116.29 (Ph ring *C*H), 117.3 (CH*C*H=CH₂), 121.2 (*C*N), 126.8, 130.4 and 130.6 (Ph ring *C*H), 131.8, 139.3 (CH*C*H=CH₂), 157.6 and 158.1 (*C*OH). HRMS (FAB): *m/z* 272.1270 ([M + Li]⁺, C₁₇H₁₅NO₂Li, calcd 272.1263).

(2R*,3S*)-2,3-Bis(4-((2-methoxyethoxy)methoxy)phenyl)pent-4-enenitrile (7). To a solution of (2*R**,3*S**)-2,3-bis-(4-hydroxyphenyl)pent-4-enenitrile (422 mg, 1.59 mmol) in mixture solvent of anhydrous CH₂Cl₂ (8 mL) and THF (4 mL) were added 2−methoxyethoxymethyl chloride (MEM chloride, 829 µl, 7.26 mmol) and *N,N*−diisopropylethylamine (2.1 mL, 12.1 mmol) consecutively. The flask was stirred under Ar gas atmosphere for 2.5 days. The solution was diluted with ethyl acetate (25 mL), then washed by water, 0.5 M HCl, NaHCO₃, and brine, dried by MgSO₄, and concentrated under vacuum. The crude product was purified by flash column chromatography (silica, ethyl acetate/hexane (1:1)) to give a clear oil. (442 mg, 60%): ¹H NMR (CDCl₃, 300 MHz) δ 3.348 (s, 3H), 3.352 (s, 3H), 3.54 (m, 4H), 3.66 (m, 1H), 3.78 (m, 4H), 4.05 (d, *J* = 6.9 Hz, 1H), 5.11 (m, 2H), 5.23 (s, 4H), 5.98 (m, 1H), 6.99 (m, 8H); ¹³C NMR (CDCl₃, 75 MHz) δ 43.3 (*C*HCN), 53.8 (*C*HCH=CH₂), 59.0 (O*C*H₃), 67.7 and 67.8 (*C*H₂CH₂OCH₃), 71.6 (CH₂*C*H₂OCH₃), 93.46 and 93.50 (PhO*C*H₂O), 116.3 and 116.4 (Ph ring *C*H), 117.9 (CH*C*H=CH₂), 119.9 (*C*N), 127.1, 129.5 and 129.6 (Ph ring *C*H), 136.9 (CH*C*H=CH₂), 156.7, 157.1.

(2R*,3S*)-2,3-Bis(4-((2-methoxyethoxy)methoxy)phenyl)-5-hydroxypentanenitrile (8). To a solution of (2*R**,3*S**)-2,3-bis(4-((2-methoxyethoxy)methoxy)phenyl)pent-4-enenitrile (442 mg, 1.0 mmol) in dry THF was added 1M BH₃·THF (1.2 mL) dropwise at 0 °C. The mixture was allowed to warm to room temperature slowly and stirred under argon gas for 6 h. After quenching with water (2 mL), to the flask were added 3 M NaOH (4 mL) and 35% H₂O₂ (4 mL) at 0 °C. The resulting mixture was stirred for 1 h in ice bath. The solution was diluted by ethyl acetate (40 mL), then washed by water and brine and dried over MgSO₄. The residue, after evaporation, was chromatographed over silica using ethyl acetate/hexane (3:1) as eluent to give a clear oil. (248 mg, 54%): 1H NMR (CDCl₃, 300 MHz) δ 1.96 (m, 2H), 3.16 (m, 1H), 3.35 (s, 6H), 3.33−3.57 (m, 2H), 3.54 (m, 4H), 3.79 (m, 4H), 3.99 (d, *J* = 7.2 Hz, 1H), 5.22 (s, 4H), 6.97 (m, 8H); ¹³C NMR (CDCl₃, 75 MHz) δ 35.8 (*C*HCH₂CH₂OH), 43.9 (*C*HCN), 46.5 (CH₂*C*H₂OH), 59.1 (O*C*H₃), 60.2 (CH₂*C*H₂OH), 67.79 and 67.83 (*C*H₂OCH₃), 71.69 and 71.72 (CH₂*C*H₂OCH₃), 93.5 and 93.6 (O*C*H₂O), 116.38 and 116.54 (Ph ring *C*H), 120.1 (*C*N), 127.7, 129.44 and 129.58 (Ph ring *C*H), 132.1, 156.8, 157.1. HRMS (FAB): *m/z* 466.2428 ([M + Li]⁺, C₂₅H₃₃NO₇Li, calcd 466.2417).

(3R,4S)-3,4-Bis(4-((2-methoxyethoxy)methoxy)phenyl)-4-cyanobutyl 4-methylbenzenesulfonate (9). To a solution of (2*R**,3*S**)-2,3-bis(4-((2-methoxyethoxy)methoxy)phenyl)-5−hydroxypentanenitrile (248 mg, 0.54 mmol) in CH₂Cl₂ (10 mL) were added *p*-toluenesulfonyl chloride (113 mg, 0.59 mmol) and pyridine (2 mL, 24.7 mmol) consecutively. The reaction mixture was stirred under Ar atmosphere at room temperature for 26 h. The solution was diluted with ethyl acetate (30 mL), then washed by water, 10% citric acid (3 × 20 mL), 0.1 M HCl, and brine, dried over MgSO₄, and concentrated. The crude product was purified by flash column chromatography (silica, ethyl acetate/hexane (3:1)) to give a clear oil. (122 mg, 37%): 1H NMR (CDCl₃, 300 MHz) δ 2.02−2.13 (m, 2H), 2.44 (s, 3H), 3.07 (m, 1H), 3.370 (s, 3H), 3.374 (s, 3H), 3.56 (m, 4H), 3.71 (m, 1H), 3.82 (m, 4H), 3.91 (d, *J* = 7.2 Hz, 1H), 3.99 (m, 1H), 5.23 (s, 2H), 5.25 (s, 2H), 6.87 (b s, 4H), 6.96 (s, 4H), 7.29 (d, *J* = 8.4 Hz, 2H), 7.66 (d, *J* = 8.4 Hz, 2H); ¹³C NMR (CDCl₃, 75 MHz) δ 21.8 (Ph*C*H₃), 32.5 (*C*HCH₂CH₂O), 43.6 (*C*HCN), 46.0 (*C*H₂CH₂OS), 59.2 (O*C*H₃), 67.8 (*C*H₂CH₂OS), 67.9 (CH₂*C*H₂OCH₃), 71.74 and 71.77 (*C*H₂CH₂OCH₃), 93.61 and 93.58 (O*C*H₂O), 116.5 and 116.7 (Ph ring *C*H), 119.7 (*C*N), 127.1, 128.0, 129.4, 129.5, 130.0, 130.6, 132.9 (*C*CH₃), 145.1 (OS*C*), 157.1, 157.3. HRMS (FAB): *m/z* 620.2492 ([M + Li]⁺, C₃₂H₃₉NO₉SLi, calcd 620.2506).

(2R*,3S*)-2,3-Bis(4-((2-methoxyethoxy)methoxy)phenyl)-5-fluoropentanenitrile (10). To a solution of (2*R**,3*S**)-2,3-bis(4-((2-methoxyethoxy)methoxy)phenyl)-5−hydroxypen-

tanenitrile (54 mg, 0.12 mmol) in dry CH₂Cl₂ (10 mL) was added (diethylamino)sulfur trifluoride (DAST, 200 µL, 1.53 mmol) dropwise at −94 °C. The mixture was stirred under Ar gas and allowed to warm to room-temperature overnight. The flask was cooled to 0 °C again and quenched by saturated NaHCO₃. The solution was diluted with ethyl acetate (30 mL), then washed by brine solution (2 × 20 mL), dried over MgSO₄, and concentrated. The crude product was chromatographed over silica using ethyl acetate/hexane (3:1) as eluent to give a pale yellow oil. (28 mg, 52%): ¹H NMR (CDCl₃, 300 MHz) δ 1.98−2.24 (m, 2H), 3.19 (m, 1H), 3.374 (s, 3H), 3.379 (s, 3H), 3.56 (m, 4H), 3.82 (m, 4H), 4.0 (d, *J* = 7.2 Hz, 1H), 4.07−4.51 (m, 2H), 5.26 (s, 4H), 7.00 (m, 8H); ¹³C NMR (CDCl₃, 75 MHz) δ 34.1 (d, *J*_CF = 20.5 Hz, *C*H₂CH₂F), 43.8 (*C*HCN), 46.1 (d, *J*_CF = 4.5 Hz, *C*HCH₂CH₂F), 59.2 (*C*H₂OCH₃), 67.90 and 67.97 (*C*H₂CH₂OCH₃), 71.77 and 71.80 (*C*H₂CH₂OCH₃), 81.5 (d, *J*_CF = 164.0 Hz, CH₂*C*H₂F), 93.61 and 93.67 (O*C*H₂O), 116.5 and 116.7 (Ph ring *C*H), 119.9 (*C*N), 127.4, 129.5 and 129.7 (Ph ring *C*H), 131.3, 157.1, 157.3. R_f = 0.50 (silica, ethyl acetate: hexane = 3:1). HRMS (FAB): *m/z* 468.2372 ([M + Li]⁺, C₂₅H₃₂FNO₆Li, calcd 468.2374).

Estrogen Receptor Binding Affinity. The relative binding affinity was obtained by a competitive radiometric binding assay using 10 nM [³H]estradiol as tracer and purified full−length human ERα and ERβ, following previously published procedures.[33,34] Incubations were done at 0 °C for 18−24 h, and hydroxyapatite was used to absorb the purified receptor−ligand complexes. The binding affinities are given relative to estradiol [RBA E₂ = 100]. The RBA values are reported as the average of two determinations ± the range.

Radiochemical Synthesis. 16α-[¹⁸F]Fluoroestradiol-17β ([¹⁸F]FES) was prepared according to literature methods.[44,58,59]

(2R*,3S*)-5-[¹⁸F]Fluoro-2,3-bis(4-hydroxyphenyl)pentanenitrile ([¹⁸F]FEDPN). [18F]Fluoride, trapped on a resin (BioRad AG-1X8, 100−200 mesh), was eluted with ca. 500 µL of 0.02 M K₂CO₃ prior to use. A resin-treated water containing the [¹⁸F]fluoride anion (100−250 mCi) was transferred to a Vacutainer (Becton Dickinson, Franklin Lakes, NJ) containing Kryptofix [2.2.2] (1.1 mg per 100 µL of treated water). The water was removed by azeotropic distillation at 110 °C under a gentle stream of nitrogen with successive addition of three (0.5 mL) aliquots of acetonitrile. During the final evaporation the Vacutainer was removed from the oil bath when the final volume reached about 100 µL. Evaporation to dryness of the residue was conducted at room temperature. The resolubilized [¹⁸F]fluoride anion was dissolved in 400 µL of anhydrous acetonitrile and transferred to a 10-mL Pyrex brand tube with screw cap containing 2.3−3.5 mg of (3*R*,4*S*)-3,4-bis(4-((2-methoxyethoxy)methoxy)phenyl)-4-cyanobutyl 4-methylbenzenesulfonate (**9**). A 3 mm glass bead was also added to the tube for a more homogeneous heat distribution during the heating and the tube capped firmly. The mixture was vortexed and reacted under microwave irradiations on medium power (60 W) for 35 s. After cooling, 100 µL of 3 M HCl was added and the mixture heated for 3 min in an oil bath at 110 °C.

The crude reaction mixture was diluted with water to about 6 mL. Solid-phase purification was performed using a Waters (HLB-6 cc) OASIS cartridge previously rinsed with 6 mL of methanol and 2 × 6 mL of MilliQ water. After the radioactive sample had been applied, the cartridge was rinsed with an additional 2 × 6 mL water to eliminate unreacted fluoride and salts, then the radiolabeled product was eluted with ethanol (2 × 3 mL). When the evaporation of ethanol was nearly complete, the residue was taken up in a mixture of 1.6 mL of 20% ethanol in water and then purified by a semipreparative HPLC (Chromanetics, Partisil ODS-3, 100×10 mm, 5 µm, MeCN:EtOH:H₂O (2:20:78), 3 mL/min). The radioactive peak corresponding to the product was detected by the radioactivity monitor 15−19 min after injection and was collected for further study. The total reaction and purification time was less than 110 min; decay-corrected radiochemical yield was between 1.2% and 8.5% (*n* = 4). Radio-TLC showed that the Rf of the intermediate compound, (2*R**,3*S**)-2,3-bis(4-((2-methoxyethoxy)-

methoxy)phenyl)-5-[^{18}F]fluoropentanenitrile ([^{18}F]**10**), was 0.49 and the R$_f$ of [^{18}F]FEDPN was 0.58.

Radiochemical Purity and Specific Activity. The radiochemical purity of [^{18}F]FEDPN was determined by analytical HPLC column (Alltech, Econosil C18 column, 250 × 4.6 mm, 10 µm; 0.1 M formate:MeCN (60:40) at a flow rate of 1.5 mL/min) and found to be greater than 99%. By comparison of the integrated sample UV signal with a calibrated compound **5** mass/UV absorbance curve, the specific activity was determined to be >3100 Ci/mmol at the end of synthesis. No cold mass was detected in any UV chromatograms, and the detection limit of the UV detector was 0.5 ppm in our system. The identity of the tracer was confirmed by the coelution of [^{18}F]FEDPN with nonradioactive standard **5** on the analytical HPLC system. Retention time for [^{18}F]FEDPN was 6.9 min.

Biodistribution Studies. In the first biodistribution study, immature female Sprague-Dawley rats (44−56 g, 21−24 days old, $n = 5$ per time point) were used for evaluation of uptake due to their low level of endogenous estrogens and estrogen receptor rich uterine tissue.[32] The ^{18}F-labeled FEDPN was concentrated in vacuo, redissolved in ethanol, and diluted with isotonic saline to give final 20% ethanol/saline solution. Anesthetized rats under isoflurane/O$_2$ were injected in the tail vein with 20 µCi of the labeled compound in a volume of 150 µL. One set of animals was also coinjected with 8 µg of estradiol (E$_2$) to block uptake mediated by the estrogen receptor. At selected time points postinjection (30 min, 1 h, and 2 h), rats were sacrificed. Blood and organs were removed, blotted, weighed, and counted in a Gamma 8000 well counter along with a standard dilution of the injectate. Uptake was calculated as percent injected dose (%ID) per gram and per organ. Blood weight is assumed to be 7% body weight (BW), muscle 41% BW, and bone 10.9 BW.

In the second biodistribution study, female estrogen receptor- knock-out (αERKO) and estrogen receptor-β knock-out (βERKO) mice (ca. 22 g, 6−8 weeks old, $n = 3$ each per time point) were used to determine whether the labeled estrogen ligand shows any subtype selectivity. The ERKO mice were allowed to recover from the stress of shipping for 48 h, and the estrous cycle was checked by swabbing vagina at 72 h postarrival. Attempts were made to stage these animals to a nonestrus condition for the biodistribution study. The mice were immediately placed on a special chow which was estrogen free in order to decrease their circulating estrogens. In the first case, nine each of αERKO and βERKO mice in a nonestrus stage were each injected with 11 µCi of [^{18}F]FEDPN (130 µL of 10% ethanol/saline). The remaining mice were kept in the same cage, in the hope that they would begin cycling together; however, we ended up with all of αERKO mice cycling together. Nine of the αERKO mice and two of the βERKO mice that were cycling with them were injected with 13 µCi of [^{18}F]-FES (100 µL of 10% ethanol/saline) and sacrificed (αERKO − 30 min, 1 and 2 h ($n = 3$ each); βERKO − 30 min ($n = 2$)).

Unfortunately, the repeated vaginal swabbing in some mice used to stage the estrous cycle seemed to induce false pregnancy. Even though these mice were not swabbed for an additional 9 days, they did not come out of pseudopregnancy. As a result, the biodistribution study of [^{18}F]FES was completed by employing βERKO mice in estrus ($n = 3$ each at 30 min, 1 h, 2 h). Three serum samples of βERKO (during estrus) and normal BALC/c mice were sent out for the measurement of circulating estradiol level.

Supporting Information Available: Additional experimental details. This material is available free of charge via the Internet at http://pubs.acs.org.

References

(1) Katzenellenbogen, B. S.; Katzenellenbogen, J. A. Estrogen receptor transcription and transactivation. Estrogen receptor alpha and estrogen receptor beta. Regulation by selective estrogen receptor modulators and importance in breast cancer. *Breast Cancer Res.* [online computer file] **2000**, *2*, 335−344.
(2) Santen, R. J.; Manni, A.; Harvey, H.; Redmond, C. Endocrine treatment of breast cancer in women. *Endocr. Rev.* **1990**, *11*, 221−265.
(3) Santen, R. J.; Harvey, H. A. Use of aromatase inhibitors in breast carcinoma. *Endocr.-Related Cancer* **1999**, *6*, 75−92.
(4) McGuire, A. H.; Dehdashti, F.; Siegel, B. A.; Lyss, A. P.; Brodack, J. W.; Mathias, C. J.; Mintun, M. A.; Katzenellenbogen, J. A.; Welch, M. J. Positron tomographic assessment of 16 alpha-[^{18}F] fluoro-17 beta-estradiol uptake in metastatic breast carcinoma. *J. Nuclear Med.* **1991**, *32*, 1526−1531.
(5) Dehdashti, F.; Mortimer, J. E.; Siegel, B. A.; Griffeth, L. K.; Bonasera, T. J.; Fusselman, M. J.; Detert, D. D.; Cutler, P. D.; Katzenellenbogen, J. A.; Welch, M. J. Positron tomographic assessment of estrogen receptors in breast cancer: comparison with FDG-PET and in vitro receptor assays. *J. Nuclear Med.* **1995**, *36*, 1766−1774.
(6) Katzenellenbogen, J. A. Estrogen and progestin radiopharmaceuticals for imaging breast cancer. *Estrogens, Progestins, Their Antagonists* **1997**, *1*, 197−242.
(7) Katzenellenbogen, J. A. Receptor imaging of tumors (nonpeptide). *Handbook Radiopharm.* **2003**, 715−750.
(8) Dehdashti, F.; Flanagan, F. L.; Mortimer, J. E.; Katzenellenbogen, J. A.; Welch, M. J.; Siegel, B. A. Positron emission tomographic assessment of "metabolic flare" to predict response of metastatic breast cancer to antiestrogen therapy. *Eur. J. Nuclear Med.* **1999**, *26*, 51−56.
(9) Mortimer, J. E.; Dehdashti, F.; Siegel, B. A.; Trinkaus, K.; Katzenellenbogen, J. A.; Welch, M. J. Metabolic flare: indicator of hormone responsiveness in advanced breast cancer. *J. Clin. Oncol.* **2001**, *19*, 2797−2803.
(10) Kuiper, G. G.; Enmark, E.; Pelto-Huikko, M.; Nilsson, S.; Gustafsson, J. A. Cloning of a novel receptor expressed in rat prostate and ovary. *Proc. Natl. Acad. Sci. U. S. A.* **1996**, *93*, 5925−5930.
(11) Enmark, E.; Gustafsson, J. A. Estrogen receptor β − a novel receptor opens up new possibilities for cancer diagnosis and treatment. *Endocr.-Related Cancer* **1998**, *5*, 213−222.
(12) Kuiper, G. G. J. M.; Carlsson, B.; Grandien, K.; Enmark, E.; Haeggblad, J.; Nilsson, S.; Gustafsson, J.-A. Comparison of the ligand binding specificity and transcript tissue distribution of estrogen receptors α and β. *Endocrinology* **1997**, *138*, 863−870.
(13) Kuiper, G. G.; Gustafsson, J. A. The novel estrogen receptor-beta subtype: potential role in the cell- and promoter-specific actions of estrogens and anti-estrogens. *FEBS Lett.* **1997**, *410*, 87−90.
(14) Pettersson, K.; Gustafsson, J. A. Role of estrogen receptor beta in estrogen action. *Annu Rev Physiol* **2001**, *63*, 165−192.
(15) Hall, J. M.; McDonnell, D. P. The estrogen receptor β-isoform (ERβ) of the human estrogen receptor modulates ERα transcriptional activity and is a key regulator of the cellular response to estrogens and antiestrogens. *Endocrinology* **1999**, *140*, 5566−5578.
(16) Nilsson, S.; Makela, S.; Treuter, E.; Tujague, M.; Thomsen, J.; Andersson, G.; Enmark, E.; Pettersson, K.; Warner, M.; Gustafsson, J. A. Mechanisms of estrogen action. *Physiological Rev.* **2001**, *81*, 1535−1565.
(17) Roger, P.; Sahla, M. E.; Makela, S.; Gustafsson, J. A.; Baldet, P.; Rochefort, H. Decreased expression of estrogen receptor β protein in proliferative preinvasive mammary tumors. *Cancer Res.* **2001**, *61*, 2537−2541.
(18) Palmieri, C.; Cheng, G. J.; Saji, S.; Zelada-Hedman, M.; Warri, A.; Weihua, Z.; Van Noorden, S.; Wahlstrom, T.; Coombes, R. C.; Warner, M.; Gustafsson, J. A. Estrogen receptor beta in breast cancer. *Endocr.-Related Cancer* **2002**, *9*, 1−13.
(19) Speirs, V.; Carder, P. J.; Lansdown, M. R. J. Oestrogen receptor beta: how should we measure this? *Br. J. Cancer* **2002**, *87*, 687; author reply 688−689.
(20) Omoto, Y.; Kobayashi, S.; Inoue, S.; Ogawa, S.; Toyama, T.; Yamashita, H.; Muramatsu, M.; Gustafsson, J. A.; Iwase, H. Evaluation of oestrogen receptor β wild-type and variant protein expression, and relationship with clinicopathological factors in breast cancers. *Eur. J. Cancer* **2002**, *38*, 380−386.

(21) Meyers, M. J.; Sun, J.; Carlson, K. E.; Marriner, G. A.; Katzenellenbogen, B. S.; Katzenellenbogen, J. A. Estrogen Receptor-b Potency-Selective Ligands: Structure−Activity Relationship Studies of Diarylpropionitriles and Their Acetylene and Polar Analogues. *J. Med. Chem.* **2001**, *44*, 4230−4251.

(22) Katzenellenbogen, J. A.; Welch, M. J.; Dehdashti, F. The development of estrogen and progestin radiopharmaceuticals for imaging breast cancer. *Anticancer Res.* **1997**, *17*, 1573−1576.

(23) Ryberg, P.; Matsson, O. The Mechanism of Base-Promoted HF Elimination from 4-Fluoro-4-(4-nitrophenyl)butan-2-one Is E1cB. Evidence from Double Isotopic Fractionation Experiments. *J. Org. Chem.* **2002**, *67*, 811−814.

(24) Ryberg, P.; Matsson, O. The Mechanism of Base-Promoted HF Elimination from 4-Fluoro-4-(4′-nitrophenyl)butan-2-one: A Multiple Isotope Effect Study Including the Leaving Group [18F/19F] KIE. *J. Am. Chem. Soc.* **2001**, *123*, 2712−2718.

(25) Lee, K. C.; Lee, S.-Y.; Choe, Y. S.; Chi, D. Y. Metabolic stability of [18F]fluoroalkylbiphenyls. *Bull. Korean Chem. Soc.* **2004**, *25*, 1225−1230.

(26) Verkerk, U.; Fujita, M.; Dzwiniel, T. L.; McDonald, R.; Stryker, J. M. Tetrakis(2-hydroxyphenyl)ethene and Derivatives. A Structurally Preorganized Tetradentate Ligand System for Polymetallic Coordination Chemistry and Catalysis. *J. Am. Chem. Soc.* **2002**, *124*, 9988−9989.

(27) Lubczyk, V.; Bachmann, H.; Gust, R. Investigations on Estrogen Receptor Binding. The Estrogenic, Antiestrogenic, and Cytotoxic Properties of C2−Alkyl-Substituted 1,1-Bis(4-hydroxyphenyl)-2-phenylethenes. *J. Med. Chem.* **2002**, *45*, 5358−5364.

(28) Li, T. T.; Wu, Y. L. Facile regio- and stereoselective total synthesis of racemic aklavinone. *J. Am. Chem. Soc.* **1981**, *103*, 7007−7009.

(29) Kulkarni, P. P.; Kadam, A. J.; Mane, R. B.; Desai, U. V.; Wadgaonkar, P. P. Demethylation of methyl aryl ethers using pyridine hydrochloride in solvent-free conditions under microwave irradiation. *J. Chem. Res., Synop.* **1999**, 394−395.

(30) Gates, M.; Tschudi, G. Synthesis of morphine. *J. Am. Chem. Soc.* **1956**, *78*, 1380−1393.

(31) Fredriksson, A.; Stone-Elander, S. Rapid microwave-assisted cleavage of methyl phenyl ethers: new method for synthesizing desmethyl precursors and for removing protecting groups. *J. Labelled Compd Radiopharm.* **2002**, *45*, 529−538.

(32) Vijaykumar, D.; Al-Qahtani, M. H.; Welch, M. J.; Katzenellenbogen, J. A. Synthesis and biological evaluation of a fluorine-18 labeled estrogen receptor-α selective ligand: [18F] propyl pyrazole triol. *Nuclear Med. Biol.* **2003**, *30*, 397−404.

(33) Carlson, K. E.; Choi, I.; Gee, A.; Katzenellenbogen, B. S.; Katzenellenbogen, J. A. Altered ligand binding properties and enhanced stability of a constitutively active estrogen receptor: evidence that an open pocket conformation is required for ligand interaction. *Biochemistry* **1997**, *36*, 14897−14905.

(34) Katzenellenbogen, J. A.; Johnson, H. J., Jr.; Myers, H. N. Photoaffinity labels for estrogen binding proteins of rat uterus. *Biochemistry* **1973**, *12*, 4085−4092.

(35) Stone-Elander, S.; Elander, N. Microwave applications in radiolabeling with short-lived positron-emitting radionuclides. *J. Labelled Compd Radiopharm.* **2002**, *45*, 715−746.

(36) Ponde, D. E.; Dence, C. S.; Schuster, D. P.; Welch, M. J. Rapid and reproducible radiosynthesis of [18F] FHBG. *Nuclear Med. Biol.* **2004**, *31*, 133−138.

(37) Choe, Y. S.; Lidstroem, P. J.; Chi, D. Y.; Bonasera, T. A.; Welch, M. J.; Katzenellenbogen, J. A. Synthesis of 11b-[18F]Fluoro-5α-dihydrotestosterone and 11b-[18F]Fluoro-19-nor-5α-dihydrotestosterone: Preparation via Halofluorination-Reduction, Receptor Binding, and Tissue Distribution. *J. Med. Chem.* **1995**, *38*, 816−825.

(38) Sasaki, M.; Fukumura, T.; Kuwabara, Y.; Yoshida, T.; Nakagawa, M.; Ichiya, Y.; Masuda, K. Biodistribution and breast tumor uptake of 16a-[18F]-fluoro-17β-estradiol in rat. *Ann. Nuclear Med.* **2000**, *14*, 127−130.

(39) Choe, Y. S.; Bonasera, T. A.; Chi, D. Y.; Welch, M. J.; Katzenellenbogen, J. A. 6α-[18F]Fluoroprogesterone: synthesis via halofluorination-oxidation, receptor binding and tissue distribution. *Nuclear Med. Biol.* **1995**, *22*, 635−642.

(40) Lubahn, D. B.; Moyer, J. S.; Golding, T. S.; Couse, J. F.; Korach, K. S.; Smithies, O. Alteration of reproductive function but not prenatal sexual development after insertional disruption of the mouse estrogen receptor gene. *Proc. Natl. Acad. Sci. U. S. A.* **1993**, *90*, 11162−11166.

(41) Krege, J. H.; Hodgin, J. B.; Couse, J. F.; Enmark, E.; Warner, M.; Mahler, J. F.; Sar, M.; Korach, K. S.; Gustafsson, J.-A.; Smithies, O. Generation and reproductive phenotypes of mice lacking estrogen receptor β. *Proc. Natl. Acad. Sci. U. S. A.* **1998**, *95*, 15677−15682.

(42) Nilsson, S.; Kuiper, G.; Gustafsson, J.-A. ERβ: a novel estrogen receptor offers the potential for new drug development. *Trends Endocrinol. Metabol.* **1998**, *9*, 387−395.

(43) Jonson, S. D.; Bonasera, T. A.; Dehdashti, F.; Cristel, M. E.; Katzenellenbogen, J. A.; Welch, M. J. Comparative breast tumor imaging and comparative in vitro metabolism of 16α-[18F]-fluoroestradiol-17β and 16β-[18F]fluoromoxestrol in isolated hepatocytes. *Nuclear Med. Biol.* **1998**, *26*, 123−130.

(44) Kiesewetter, D. O.; Kilbourn, M. R.; Landvatter, S. W.; Heiman, D. F.; Katzenellenbogen, J. A.; Welch, M. J. Preparation of four fluorine-18-labeled estrogens and their selective uptakes in target tissues of immature rats. *J. Nuclear Med.* **1984**, *25*, 1212−1221.

(45) Katzenellenbogen, J. A.; Mathias, C. J.; Vanbrocklin, H. F.; Brodack, J. W.; Welch, M. J. Titration of the in vivo uptake of 16α-[18F]fluoroestradiol by target tissues in the rat: competition by tamoxifen, and implications for quantitating estrogen receptors in vivo and the use of animal models for receptor-binding radiopharmaceutical development. *Nuclear Med. Biol.* **1993**, *20*, 735−745.

(46) Mathias, C. J.; Welch, M. J.; Katzenellenbogen, J. A.; Brodack, J. W.; Kilbourn, M. R.; Carlson, K. E.; Kiesewetter, D. O. Characterization of the uptake of 16α-([18F]fluoro)-17β-estradiol in DMBA-induced mammary tumors. *Nuclear Med. Biol.* **1987**, *14*, 15−25.

(47) McElvany, K. D.; Carlson, K. E.; Katzenellenbogen, J. A.; Welch, M. J. Factors affecting the target site uptake selectivity of estrogen radiopharmaceuticals: serum binding and endogenous estrogens. *J. Steroid Biochem.* **1983**, *18*, 635−641.

(48) Couse, J. F.; Korach, K. S. Estrogen receptor null mice: what have we learned and where will they lead us? *Endocr. Rev.* **1999**, *20*, 358−417.

(49) Couse, J. F.; Curtis, S. W.; Washburn, T. F.; Lindzey, J.; Golding, T. S.; Lubahn, D. B.; Smithies, O.; Korach, K. S. Analysis of transcription and estrogen insensitivity in the female mouse after targeted disruption of the estrogen receptor gene. *Mol. Endocrinol.* **1995**, *9*, 1441−1454.

(50) Hewitt, S. C.; Couse, J. F.; Korach, K. S. The estrogen receptor knock-out mouse model. *Hormone Replacement Therapy and Cardiovascular Disease: The Current Status of Research and Practice [Expert Workshop, London, United Kingdom, Oct. 13−16, 2000]*; Parthenon Publishing Group: New York, 2001, pp 81−86.

(51) Couse, J. F.; Lindzey, J.; Grandien, K.; Gustafsson, J.-A.; Korach, K. S. Tissue distribution and quantitative analysis of estrogen receptor-α (ERα) and estrogen receptor-β (ERβ) messenger ribonucleic acid in the wild-type and ERα-knockout mouse. *Endocrinology* **1997**, *138*, 4613−4621.

(52) Emmen, J. M. A.; Korach, K. S. Estrogen receptor knockout mice: phenotypes in the female reproductive tract. *Gynecol. Endocrinol.* **2003**, *17*, 169−176.

(53) Vanbrocklin, H. F.; Pomper, M. G.; Carlson, K. E.; Welch, M. J.; Katzenellenbogen, J. A. Preparation and evaluation of 17-ethynyl-substituted 16α-[18F]fluoroestradiols: selective receptor-based PET imaging agents. *Nuclear Med. Biol.* **1992**, *19*, 363−374.

(54) Carlson, K. E.; Katzenellenbogen, J. A. Unpublished results.

(55) Malamas, M. S.; Manas, E. S.; McDevitt, R. E.; Gunawan, I.; Xu, Z. B.; Collini, M. D.; Miller, C. P.; Dinh, T.; Henderson, R. A.; Keith, J. C., Jr.; Harris, H. A. Design and Synthesis of Aryl Diphenolic Azoles as Potent and Selective Estrogen Receptor-β Ligands. *J. Med. Chem.* **2004**, *47*, 5021−5040.

(56) De Angelis, M.; Stossi, F.; Carlson, K. A.; Katzenellenbogen, B. S.; Katzenellenbogen, J. A. Indazole Estrogens: Highly Selective Ligands for the Estrogen Receptor β. *J. Med. Chem.* **2005**, *48* (4), 1132−1144.

(57) Dence, C. S.; Mishani, E.; McCarthy, T. J.; Welch, M. J. Evaluation of a microwave cavity for the synthesis of PET radiopharmaceuticals. *J. Labelled Compd Radiopharm.* **1995**, *37*, 115−117.

(58) Brodack, J. W.; Kilbourn, M. R.; Welch, M. J.; Katzenellenbogen, J. A. NCA 16α-[18F]fluoroestradiol-17β: the effect of reaction vessel on fluorine-18 resolubilization, product yield, and effective specific activity. *Appl. Radiat. Isotopes* **1986**, *37*, 217−221.

(59) Brodack, J. W.; Kilbourn, M. R.; Welch, M. J.; Katzenellenbogen, J. A. Application of robotics to radiopharmaceutical preparation: controlled synthesis of fluorine-18 16α-fluoroestradiol-17β. *J. Nuclear Med.* **1986**, *27*, 714−721.